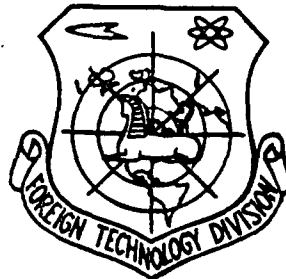AD-A206 782

FOREIGN TECHNOLOGY DIVISION

ACTA AERONAUTICA ET ASTRONAUTICA SINICA

(Selected Articles)

DTIC
ELECTE
APR 0 7 1989
S D
D

89 4 03 044

HUMAN TRANSLATION

FTD-ID(RS)T-0942-88   15 February 1989

MICROFICHE NR: FTD-89-C-000089

ACTA AERONAUTICA ET ASTRONAUTICA SINICA
(Selected Articles)

English pages: 66

Source: Hangkong Xuebao, Vol. 8, Nr. 12,
         December 1987, pp. B557-B562;
         B585-B593; B601-B610

Country of origin: China
Translated by: SCITRAN
                F33657-84-D-0165
Requester: ASD/FTD/TQIA
Approved for public release; Distribution unlimited.

TABLE OF CONTENTS

i

GRAPHICS DISCLAIMER

All figures, graphics, tables, equations, etc. merged into this
translation were extracted from the best quality copy available.

SOME ASPECTS OF NOSE-WHEEL SHIMMY AND SHIMMY DAMPER OF THE AIRCRAFT

Zhu Depei

SUMMARY

This article is aimed toward the interests of specialist
technical personnel dealing with aircraft take off and landing gear as
they concern nose wheel shimmy and measures to prevent it. It also
deals with an analysis of runway dynamics and other such similar areas
as nose wheel operation. It offers some brief comments and main
points but certainly does not constitute a detailed introduction.

I. INTRODUCTION

Modern aircraft employ, for the most part, a forward three point
type of take off and landing gear. According to statistics on 180
types of aircraft (1), with the exceptions of the use of the small
wheel barrow type wing tip auxilliary gear used on such types of
aircraft as the "Blackbird" and the B-52 as well as the rear three
point fixed type of gear employed on the Y-5 aircraft, all remaining
types employ the forward three point take off and landing gear across
the board. In reference (1), in statistics on 50 types of
helicopters, there were also 22 types which employed the forward three
point take off and landing gear.

It is possible to make a general distinction. When dealing with
aircraft which have maximum take off weights of 20 tons or less, the
majority make use of a single wheel type of nose gear. However, when
one is dealing with 20 tons and over, then, one sees the frequent
employment of dual wheel types. In the case of the C-5 aircraft, the
maximum take off weight is 363 tons, and the foward take off and
landing gear possesses four coaxial parallel wheels. In a jumbo type
transport plane, the design specifications (2) show a maximum take off
weight of 436 tons. The whole plane has 28 uniform wheels, and the
forward take off and landing gear also makes use of four parallel
wheels. On the basis of the introduction by K.G. Hancock and others
(3), when use is made of multiple wheel type forms, the Americans have
a tendency for their wheels not to turn together. At the present
time, they are still reliant on hydraulic pressure damping to prevent
shimmy.

On the basis of requirements for stability in the direction of aircraft take off runs or taxiing and for maneuverability, the forward wheels should be able to turn around to a certain directional axis and rotate freely. Because of this, it is possible to see the occurence of shimmy. Forward wheel shimmy is a severe malfunction often seen in the test production and use of aircraft. In our country, such aircraft as the J-8, Y-11, and Y-12, in their test production, and aircraft like the J-5, J-6, TY-4, and IL-28, in their normal utilization, all experienced problems with shimmy. Such U.S. aircraft as the C-119, F7U-3, and L1011, in their test production, gave rise to shimmy. Shimmy influences the control of the pilot, gives rise to structural fatigue damage, excites structural resonance, and, when it is severe, creates structural failure, leading to tragic accidents. Because of this, it is all the more necessary to prevent it.

As far as the theory of shimmy is concerned, as well as research into measures for the prevention of it, the principal references were published in the decades from the 40s to the 60s. Reference (4) has a complete introduction as well as collecting experimental results and experience inside China. Beginning in the decade of the 70s, in open publications, references on specialized topics related to shimmy tended to concentrate on the reduction of noise and the elimination of its symptoms. Shimmy had become an old subject.

Reference (5), for the first time, analyzed the influence of forward wheel shimmy reduction and damping on the stability of aircraft take off run direction. It brought out the point of view that shimmy reduction and damping should be adopted on the basis of the two considerations of the preventing of forward wheel shimmy and the insuring of stability in the direction of aircraft take off runs.

From the decade of the 50s on, the majority of large and medium type aircarft all made use of dynamic control, using control of the front wheels in order to change or maintain the direction of the aircraft's take off run. The moments of control force came from servo-hydraulic pressure operator tubes. The size of these was to be determined on the basis of a static and dynamic analysis of the aircraft's take off run. As far as forward wheel control systems are concerned, they all require the provision of hydraulic pressure damping to prevent shimmy. Because of this, they were called control

2

shimmy reduction devices. Among the references that discuss an
analysis of the dynamics of aircraft take off runs--for example,
reference (3) and reference (6)--there are frequent errors. They take
the instantaneous center of aircraft rotation to be the center of the
curvature of the track of the center of gravity. These errors had to
be dealt with. Besides this, there were also people who did not have
a thorough theoretical understanding of the concept of stability in
the direction of take off runs. This article will make a concise
clarification of these problems.

II. A SHORT INTRODUCTION TO THE THEORY OF NOSE WHEEL SHIMMY   2

Nose wheel shimmy is a type of self-exciting vibration. It is
one of the problems concerning the stability of system motion. In an
engineering analysis, the structures of take off and landing gears can
be taken and handled as linear systems, possessing a limited degree of
freedom of motion. What must be handled in a specialized manner are
the characteristics of the tires. In references on shimmy outside of
China, one often sees the use of several types of theories on shimmy
which are designated by researchers names. In the earliest days,
there were such authors as Kantrowitz (7), Carbon (8), and others who
gave a relatively clear illucidation of the phenomena of tire
deformation during shimmy. After that, reflecting differences in
hypotheses about tire deformation, the field was divided into the
point contact theory and the line theory. The former included
articles by such people as Moreland (9), Black (10), Pacejka (11),
Kelzysh (12), Carbon (8) and others. The latter included articles by
such people as McBrearity (13), Smily (14), Schlippe (15) and others.
The author of this article, after going through a detailed comparison
and contrast, reached his conclusions (4). As far as the basic
equations for all shimmy references are concerned, after making
appropriate substitutions of symbols, they are consistent. Among
these, the approximate point contact theory was consistent with a
first order approximation of the line theory. What is called the
strict point contact theory and a second order approximation of the

line theory were consistent. Reference (4) displays the comparitive relationships between symbols. As far as practical applications are concerned, second order theories are sufficient. Pacejka (11) presents the field theory of tire deformation. However, the precision of his initial data and its application in non-steady state rolling movements is exceptionally troublesome. At the time of application, it is necessary to simplify. For practical purposes, it is still possible to return to the point contact theory. Because of this, it is inappropriate to distinguish the various types of theories according to the names of authors.

Besides direct research on the characteristics of tires, there are also authors such as Rogers (16), Collins (17), and others, who take wheels and tires and make them into an integraced body. Through experiments, they measure its overall dynamic characteristics. Moreover, they take shimmy systems and view them as forming a closed loop system, studying its stability.

The theory of shimmy can be divided into linear theories and non-linear theories. These can be made into a motion stability type of problem. On the basis of the classic theories of Liopenov (phonetic transliteration), with small perturbations, from linearized assumptions leading to results which are related to stability, it is possible to make appropriate applications in actual non-linear systems. Because of this, when figuring out shimmy designs, one makes principal use of linear theories. Moreover, when adequate consideration is given to the degree of stability reserve, this is workable. As far as the standard types of forward take off and landing gear--which have adequate rigidity--are concerned, the results of shimmy theory calculations and the actual situations usually agree relatively well.

In actual occurrences of shimmy, one induces that the principal causes of them are:

1. The bending moments of the struts are not adequate, or the motion transfer rigidities of shimmy reduction systems are insufficient. For example, in the case of the F-3 aircraft, the height of the nose take off and landing gear was very great. This caused the strut rigidity to be inadequate. Also, as concerns nose wheels which have angles of directional rotation which can reach 360

degrees, control shimmy reduction systems must be installed at the top end of the struts. When this is done, the path of force transmission is too long for the moments of force of the shimmy reduction damping. This can also lead to inadequate transmission rigidity.

2. Fluids in shimmy reduction devices contain gas bubbles or gaps. These problems may be due to improper charging, or they may be due to large differences in ambient temperatures during the flight and landing process. As a result, the functioning of the fluids in the compensation chambers are also inadequate, causing problems. At such times, one should strengthen the back pressures in oil chambers and increase the functioning of pressure storage vessels in order to eliminate gaps in the internal fluids.

3. Gaps exist in the force transmission systems of shimmy reduction devices. This is due to friction damage during long term use, or it may be due to improper machining of products. It may also be created by inappropriate maintenance and repairs.

Normal shimmy can be called "tire type" shimmy. Corresponding to the several types of causes described above, one can also subdivide cases into so called "sturctural type" shimmy, "damping free travel" shimmy, or "gap type" shimmy. In another respect, shimmy can also be divided into "large angle" shimmy and "small angle" shimmy (3). Large angle shimmy is extremely violent. The lateral forces will reach the limits of the friction forces, and the tires will show the appearance of lateral drifting movements. The frequency will normally be 8 Hz ~ 10 Hz. Small angle shimmy shows a small degree of violence. The tires do not show the appearance of lateral drifting. Its frequency is relatively high. However, this type of shimmy must also be controlled.

III. PRACTICAL MEASURES FOR PREVENTING SHIMMY

As far as an explanation of the theory of shimmy is concerned, in the case of inadequate rigidity in the take off and landing gear, increasing the stability distance of the nose wheel is effective in

the prevention of shimmy. When the stability distance or metacentric height reaches the radius of the wheels, it is generally possible to avoid shimmy. However, at such a time, the strut bending moment caused by opposing forces from the surface of the ground is also very large. Because of this, the metacentric height must be limited in its increases. This is particularly true for large aircraft. In the case of the Y-12 aircraft, during its test production, it experienced the occurrence of violent shimmy. Finally, a strategy was adopted to make increases in the angle of forward slant on the take off and landing gear struts as a measure in order to increase the metacentric distance, overcoming the shimmy phenomena. The strut bending moment was also considerably increased. The effects of this were very good. Generally speaking, the value for the metacentric distance must, at least, cause the aircraft, when drifting during landings, to make the lateral movements of its tires able to overcome the various types of drag forces allowing extraction of the wheels. In order to accomplish this, it is generally necessary to select 20% or more of the diameter of the tires.

3

As far as the selection for use of coaxially turning double wheel type gear is concerned, this is advantageous for the prevention of shimmy. At such times, it is necessary to pay attention to guaranteeing that the common axle has a high torsion rigidity and small fitting tolerances or gaps. If this is not done, due to the torsional deformations of the axle or its loosening, this will increase the degree of free play in the shimmy system. Another advantage of double wheel type gears is their damage safety characteristics. However, double wheel coaxial gears are not good for the stability of the aircraft's take off run direction. They also increase the moment of turning control forces. The amount of this increase can reach approximately 50%, even reaching unacceptable levels. Another disadvantage to the adoption for use of double wheel gear in small aircraft types is that the dimensions of the wheels can be too small. This is an extreme disadvantage on rough runways. Besides this, one must also consider that, after a tire blow out, there will be created very large moments of force from lateral shimmy.

It is necessary, in liquid pressure control systems, to install pressure release valves in order to limit this type of moment of force, thus protecting the function. Also, after the explosion of a certain tire, one will lose the beneficial functioning of the dual tire coaxial turning. There is also the possibility of the occurrence of shimmy. In order to prevent tire explosions, some people put forward the actual center tire design. This will increase the weight.

It will also influence shock absorption characteristics. Due to the fact that the coaxially turning double wheel type of gear does not necessarily prevent shimmy, and it also has the various types of disadvantages explained above, in more and more cases, non-coaxially turning dual wheel type gear will be selected for use.

The measure which is most commonly used to prevent shimmy is still shimmy reduction damping devices. In the early days, multiple plate type friction damping devices were often selected for use. This type of damping is related to the size of the nose wheel or forward wheel load. In the case of all positions provided with friction damping, during installation and repair and maintenance, it is necessary to maintain between the friction faces an appropriate degree of tightness in order to supply the correct damping forces. Friction damping is not helpful in terms of the free turning of the wheels. Generally, it will not permit an excessive amount. For example, an amount not exceeding what is necessary to make the aircraft maintain a 1 degree angle of roll deviation would be acceptable.

The characteristics of hydraulic pressure damping devices compare favorably with friction damping devices. However, as was explained earlier, it is necessary to pay attention to the status of the charging in order to prevent the creation of gaps and gas bubbles. It is also necessary to pay attention to gaps in the force transmission system to maintain transmission efficiency. An ideal design should use both friction damping devices and hydraulic pressure damping devices. The former mainly prevent small angle shimmy. The latter mainly prevent large angle shimmy.

7

It is necessary to point out that damage to or cracking of damping reduction device systems can possiblly be due to the shimmy load. It can also possiblly be due to effects produced by the repeated loadings from the lateral impacts of aircraft landings. Reference (18) analyzed the problem of broken axles and the shimmy reduction devices of the J-5 aircraft. The author of this reference experienced an initial recognition that the broken axles were due to excessively large loadings given rise to by the lateral impacts of landings. Because of this, he considered a plan to "take the soft and overcome the rigid", and then drafted up plans including the use of such devices as pressure release valves in order to limit the largest hydraulic pressure drag or resistance forces. Through a suggestion by the author of this article, the author of the reference in question went through experimental verification of the fact that the broken axles were due to shimmy. Because of this, the measures which were adopted for alternative use are appropriate for changes in the amount of charge in shock absorber tubes. He carried through an increase in the turn angle of the take off and landing gear rocker arm and increased the metacentric height. Besides this, he changed the shimmy reduction system transmission ratio in order to increase damping of shimmy movement. These various measures, in field trials, have already achieved excellent results.

IV. PROBLEMS IN THE DYNAMIC ANALYSIS OF THE DIRECTION OF TAKE OFF RUNS

The stability of aircraft take off run or, in this case, landing run directions involves the discussion of a situation in which the aircraft's forward wheels and main wheels are all already in contact with the ground, in which the effects of ground surface forces form the principal factors involved, and in which aerodynamic forces--because their speed has dropped--can be ignored. Here, we will deal in particular with the stability of the direction steered by aircraft entering a field and landing. Later, we will discuss the stability of the direction steered by aircraft when entering fields for landings at large angles of attack or the stability of the direction steered by rear three point type take off and landing gears after their main wheels have touched down but while aerodynamic forces must still be considered.

8

The basic variable in the problem of the stability of direction
of aircraft runs is the angle of the direction of the run. As far as
lateral positions of the aircraft are concerned, theoretically, it is
possible to deviate from the original position in an unlimited
fashion, but this cannot possibly be stable. Besides this, one
cannot take a misunderstanding of the concept of directional stability
to be "After the disappearance of a perturbation, movement is able [19]
automatically to restore itself to the original direction of the run."

Rather, one should compare this to the classical theorem of Liaponov
(phonetic transliteration) which is understood as "It is only
necessary for a perturbation to be of a sufficiently small value, and
the value of the deviation of motion from the original direction will
be able to be smaller than a certain determined size." Finally, one
can point out that, when one has directional stability, the curvature
of the track of the motion must certainly tend toward zero. In just
the way that people, on the basis of clever skills, are able to
maintain unstable states of equilibrium, pilots are also able to   4
control aircraft with unstable directions of take off or landing run.
However, this puts them in a tense situation, and considerable
difficulties are involved.

In the references which deal with dynamic analyses of aircraft
landing and take off runs, the author of this article has discovered a
conceptual error. That is, taking the center of instantaneous
aircraft rotation to erroneously be the curvature center of the track
of the center of gravity. Fig.1 and Fig.2 are taken respectively from
reference 6, p.95, fig.1 and reference 3, p.518, fig.6. Please pay
attention in the two figures to the fact that the centripetal
acceleration at the center of gravity of the aircraft is always taken
as V^2/R. Clearly, there was no consideration given to the influence
of the acceleration of the instantaneous center point itself. Because
of this, it is only appropriate for use in situations in which the
instantaneous center or position does not change (fixed point
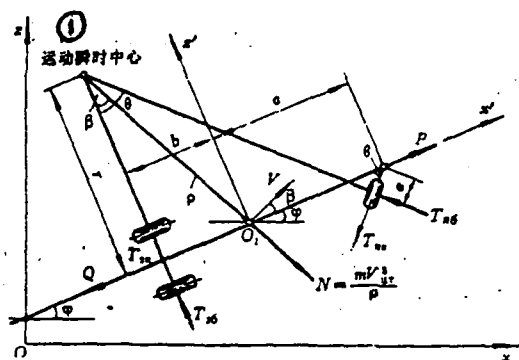rotation) or has only moved along a center of gravity ray.

Fig.1　A Diagram of the Instantaneous Center of Aircraft　Motion　and the Center of Curvature of the Center of Gravity Track　1. Center of Instantaneous Motion

Assume that, in Fig.1, a/b=5.　The angle of nose wheel shimmy motion makes a monotonic variation　$\theta = \theta_0 e^{-\lambda t}$　.　The characteristic travel length V/λ =10b, or it makes a simple harmonic variation $\theta = \theta_n \sin \omega t$.　The travel wavelength 2 π V/ ω =30b.　Then, it is easy to calculate the corresponding error brought on by ignoring the increasing speed of the instantaneous center which is approximately 10%~20%.

V. CONTROL SHIMMY REDUCTION DEVICES

Aircraft, during take off and landing runs, must go through controls in order to maintain or change the direction of their movement.　When aerodynamic effects are very small and the directional rudder has already lost its effectiveness, it is possible to select for use these methods:　(1) tractors, extending even to the use of human propulsion power;　(2) main wheel differential motion brakes;

(3) engine differential propulsion; (4) control of nose wheels or
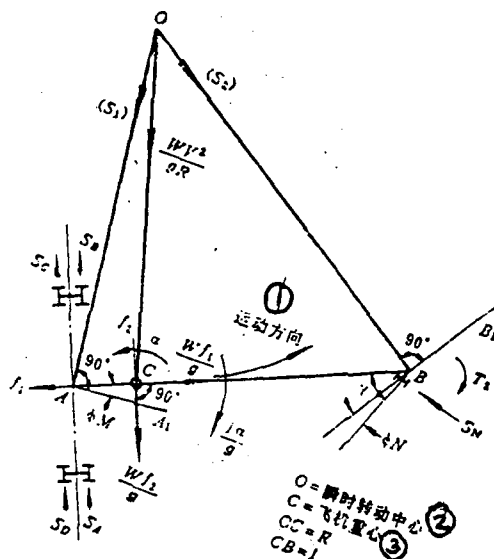tail wheels. The last three types of methods can be used together.

Fig.2 A Diagram of the Instantaneous Center of Aircraft Motion and
the Center of Curvature of the Track of the Center of Gravity 1.
Direction of Motion 2. Instantaneous Center of Rotation 3. Aircraft
Center of Gravity

Differential braking will speed up the occurrence of heat damage to
tires. Moreover, it gives rise among crew members to an annoying
"forward shock." Differential propulsion or thrust is not easy to
accurately control. Also, when one is taking off, it will cause the
loss of part of the thrust. Because of this, the most attractive is
the last type of method. With the exception of the lightest types of
aircraft, what is needed are moments of control force coming from
servomechanisms. This is called "dynamic or power control". The
design of dynamic controls must consider characteristics,
capabilities, weight and production costs. It is necessary to:

11

(1) estimate the moments of control force and control speeds; (2)
make a precise determination of the methods for preventing shimmy and
estimate the values for the moments of resistance or drag forces; (3)
estimate the value for the moments of centering force on the wheels;
(4) from the results for the various quantities we just discussed,
estimate the overall moment of control forces; (5) carry out
calculations of the control structure characteristics.

Reference (20) gives us several concrete rules for the ranges
concerned. Moreover, it also provides schematic diagrams for several
model numbers of control shimmy reduction devices. Reference (21)
provides several schematic diagrams of old style structures. Fig.3
shows the operating principles providing shimmy damping in control
shimmy reduction devices.

The precise determination of values for moments of control forces
is the problem which commands the initial interest of the designer.
He should give consideration to the several areas set out below.

In order to satisfy the requirements for control of turns in nose
wheel direction when aircraft are at rest--on the basis of equilibrium
relationships between the forces--the values for the moments of
control force are   5

$$M = M_{axle} + M_{ground} \cdot \frac{l}{l-t}$$

In this equation, M_{axle} is the moment of resistance or drag force to
the turning movement changing the direction of the axle of the wheel;
M_{ground} is the moment of resistance or drag force to the turning
movement of the wheel on the surface of the ground; l is the front to
rear distance of the forward and main wheels; t is the metacentric
height for the nose wheel(s).

In order to satisfy requirements for nose wheel control in turns
of direction when the aircraft is moving, it is possible, on the basis
of a dynamic analysis of take off and landing runs, to precisely
determine values for the moments of control force required. For
example, in the case of large aircraft, there is a requirement to be
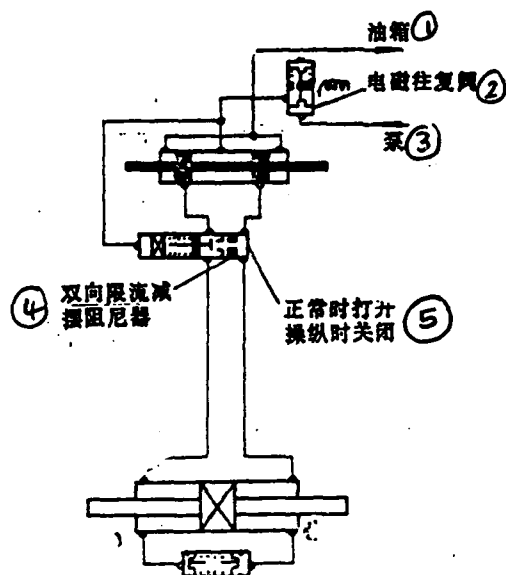able to turn 180 degrees on a runway 47.2 meters wide.

12

Fig.3 Schematic Diagram of Shimmy Damping in Control Shimmy Reduction
Devices 1. Oil Tank 2. Electromagnetic Reciprocating Valve 3. Pump
4. Dual Direction Limited Flow Shimmy Reduction Damping Device 5.
Open in Normal Situations. Closed When Controlling

     In another respect, in systems, it is possible to install
pressure release valves in order to limit the maximum angle of side
roll for wheels. As far as the status of the maximum loads on nose
wheels or forward wheels and maximum friction forces is concerned, the
maximum angle of side roll can be selected as 8 degrees. As concerns
the status of the minimum loading on nose wheels and minimum friction
forces, it is possible to select 15 degrees. In the case of excessive
side roll angles, besides increasing friction damage to the tires,
during take off and landing runs, when they run across depressions and
obstacles, they can give rise to danger. There have already been
practical examples to illustrate this. Excessively large angles of
side roll or angles of roll deviation cause tires to experience
violent vibrations, creating structural fatigue and destruction.

According to statistical data (20), the range of the overall moment of control forces is M=(0.34-0.98)tP. In this equation t is the metacentric height or stability distance. P is the load on the forward wheel. At times when the moment of control forces supplied is not sufficient--in order to increase the efficiency of the control--it is necessary to select for use together differential braking and differential thrusts.

After a precise determination of the moment of control forces, the designer is able to select hydraulic pressure, electrical, or air pressure systems. This type of selection, to a definite degree, must fit together with systems for other uses. For example, the system for raising and lowering take off and landing gear, the system for extending and retracting flaps, wheel braking systems, and so on.

VI. CONCLUSION

This article discusses the problems associated with nose wheel shimmy and shimmy reduction devices. When one considers the theory of shimmy, it is an old problem with which the profession is already well acquainted. It has not seen much new development. Shimmy reduction devices are also involved with problems which deal with quite a number of practical structures, industrial techniques, tests, applications, and maintainence. Also, one ᴖhould consider that the author of this article and co-workers have previously published specialized works on the subject (4). Because of this, in this article, which is an overall description of limited scope, I only endeavored to provide a few clues and points of importance for general consideration. Limited as it is to the knowledge of the author, I invite readers to please point out and correct what is unnecessary and obvious as well as the errors, which are difficult to avoid.

REFERENCES

[1] 卢成文、李景忠等编，简明世界飞机手册．航 空 工 业出版社，1985年12月．

[2] Fielding.J.P.,A Very Large Cargo Aircraf^t Design Project,Aircraft Engineering,Vol.55 No.9,(1983),pp 2—11.

[3] Hancock, K.G. & Person,P., Power Steering for Aircraft,Journal of the Royal Aeronautical Society,July(1952),pp 513—535.

[4] 诸德培等编著，摆振理论及防摆措施,国防工业出版 社,1984年11月．

[5] 诸德培，飞机前轮摆振问题及减摆器阻尼系数 的 选 取，西北工业大学，1962年3月．

[6] Блажлова.П.И.,Амортизация я управление Взлетно-Посадочных устройств Самолетов,Московский,Авиационный ч Институт,Москва，(1962) ．

[7] Kantrowitz,A.,Stability of CasteringWheels for Aircraft Landing Gears, NACA Rep.686,(1940).

[8] Bourcier de Carbon,Analytical Study of Shimmy of Airplane Wheels,NACA TM 1337,(1948).

[9] Moreland,W.J.,The Story of Shimmy, JAS,Vol.21,No.12,Dec.(1954),pp793—808.

[10] Black,R.J.,Comments on Syntheseis of Tire Equations for Use in Shimmy and Other Dynamic Studies,Journal of Aircraft, Vol.9,No.4,April(1972),pp 318—319.

[11] Pacejka,H.,The Wheel Shimmy Phenomenon, Ph.D.Thesis,Delft Technical Institute, Holland,Dec.(1966).

[12] Келдыш, М.В., Шимми Переднего Колеса трехколесного шасси, Труды ЦАГИ 564, (1945) ．

[13] McBrearity,J.F.,A Review of Landing Gear and Ground Loads problems, AGARD Rep.118,(1957).

[14] Smily, R.F., Correlation, Evaluation, and Extension of Linearized Theories for Tire Motion and Wheel Shimmy,NACA Rep.1299,(1957).

6

15

[15] Von Schlippe, B. & Dietrich,R., Shimmy of a Pneumatic wheel, NACA TM 1365, (1964),pp125—160,217—228.

[16] Rogers,L.C. & Brewer,H.K., Synthesis of Tire Equations for Use in Shimmy and Other Dynamic Studies,Journal of Aircraft, Vol.8,No.9, Sep.(1971), pp 689—697.

[17] Collins, R.L., Frequency Response of Tires Using the Point Contact Theory, Journal of Aircraft,Vol.9, No.6, June(1972), pp 427—432.

[18] 沙伯南、贾朝升，歼五、歼六前起落架防摆延寿改进设计，中国航空学会起落架学术会议报告，论文集第三册，编号8621—39，西安，1986年.

[19] Н.Г.马尔金著，舒伯民等译，运动稳定性理论，科学出版社，1958年8月.

[20] 诺曼·斯·柯里著，飞机试验研究中心译，起落架设计手册，即将出版。

[21] Conway,H.G.,Nose-Wheel Steering Systems, Journal of RAS, Sep.(1951), pp 586—591.

SOME ASPECTS OF NOSE-WHEEL SHIMMY AND SHIMMY DAMPER OF THE AIRCRAFT

Zhu Depei A88-29251

(*Northwestern Polytechnical University*)

Abstract

This paper discusses some aspects of nose-wheel shimmy and shimmy damper, including the dynamic analysis for taxi,and the steering for nose-gear etc., especially what the technicians in the speciality of aircraft undercarriage are concerned with.

Besides a brief review of the theories and the preventions of nose-wheel shimmy,the author also points out that there are some mistakes in the literatures dealing with the dynamic analysis of the taxi problem of aircrafts and presents some explanations to clear up them.

However,the contents consist of only some brief comments, key points or references, but not an introduction in detail.

16

SEMI-PREPARED AIRFIELD AND DESIGN OF DOUBLE-ACTION SHOCK ABSORBER
Gao Zhejun

SUMMARY

Airfields, in wars of the future, must necessarily suffer damage. After undergoing partial, localized repairs, they become semi-prepared airfields. This type of airfield, in those partial, localized areas, belong to the soft catagory. Moreover, surfaces in these local areas are very rough. When one is dealing with take off and landing gear equipped with the normal type of shock absorbers, on this type of airfield, take offs and landings will produce the appearance of high overloads, leading to the excessively early destruction of the components which connect the take off and landing gear to the aircraft. In order to satisfy the peculiar demands of using this type of airfield, this article investigates the design concepts of double action or double gas chamber shock absorbers. Moreover, as concerns their static and dynamic characteristics as well as the main parameters in the principles for their selection, it makes a relatively detailed comparative analysis. It makes a simple explanation of the standards for degree of roughness of runway surfaces and of the designs of other shock absorber arrangements appropriate for use on semi-prepared airfields.

I. SEMI-PREPARED AIRFIELDS AND DOUBLE ACTION SHOCK ABSORBERS

1. Presentation of the Problem

In modern war, it is necessary to immediately and quickly carry out repairs to restore locally damaged sections of airfields. This type of speedy repair and restoration of localized areas produces areas in the weak or soft catagory. Moreover, their surfaces are very rough. They are not the same as completely undamaged hard runway surfaces. Because of this, they are called semi-prepared airfields.

Besides this, in order to provide military supplies and equipment to units on the front lines, it is necessary that the front line support aircraft maintain a constant aerial shuttle. Due to the dispersion of the battle, the supplying of this type of aircraft utilization can only be accomplished by the rapid construction of

air'ields. These are also "soft" airfields with very rough surfaces.

17

If one wants to make aircraft able to utilize this type of airfield, then, take off and landing gear designs must satisfy the following two requirements:

(1) It is required that the take off and landing gear tires have adequate flotation or buoyancy characteristics. This becomes possible through the use of multiple wheels. The spacing distance between the wheels is increased. Tire inflation pressures are reduced. The realization of these objectives involves the use of such measures as selecting for use small diameter wheel rims and special use tires with wide cross sections. When aircraft roll over small bumps on runway surfaces, the use of this type of tire makes it possible, through the deformation of the body of the tire itself, to make appropriate reductions in the peak values of impact loads from the surface of the ground, thus raising the absorption capabilities of the tires.

(2) When aircraft roll on the surface of the ground and go over small bumps or depressions, it is required that the take off and landing gear have even better shock absorbing characteristics in order to reduce the peak values of loading from ground surface impacts and structural overloads, increasing the actual useful life of the components connecting the take off and landing gear to the aircraft.

As far as the resolution in design of problems like the ones discussed above is concerned, it makes possible a very wide scope of aircraft utilization, which has strategic significance.

2. Developmental History and the Path to Resolution

Outside of China, at the end of the decade of the 50s and the begining of the decade of the 60s, one already saw the start of research into this area. For example, in the decade of the 60s, the U.S. carried out extensive research on the OV-1 Mohawk and OV-10A Bronco aircraft in order to precisely determine the effects of loading on take off and landing gear dynamics during the utilization of rough runway surfaces. In the middle of the 1960s, they carried out research on the load acceptance capabilities of the C-5A aircraft when

used on rough runway surfaces. In recent days, the U.K. astronautical organization, on its Jaguar "American Leopard", and the U.S., on its Navy aircarft which was refitted to become the F/A-18L Air Force type of aircraft, for utilization on rough runway surfaces, have acheived clear design results, making this area of technology suitable for wide ranging applications.

Due to the selection of the tires, there are limits imposed by the aircraft structural spaces. In order to resolve the problem of the utilization of aircraft on rough runway surfaces, people principally placed their hopes in shock absorber design.

As far as the normal type of oil-gas shock absorber is concerned, from full extension to the stopping of the aircraft and from the stopping of the aircraft to complete compression, the compression ratios which were chosen for use were, respectively, 4:1 and 3:1. Normally, in the interval between stopped aircraft with an overload of 1.0 and the rolling overload of 2.0, shock absorbers only supply a very small amount of travel. They receive very small amounts of energy from ground surface impacts, causing hard impact overloads. The larger is the degree of slope for the part of the curve above the loading curve for a stopped aircraft and stationary shock absorbers the larger is the peak value of overloading. This type of take off and landing gear is only suitable for use on smooth concrete runway surfaces.

As far as aircraft which are equipped with double action shock absorbers are concerned, when they are rolling on the surface of the ground, they have adequate shock absorbing capabilities. They receive the energy of ground surface shocks from this type of rough runway surface, and they are capable of greatly reducing the peak values of surface impact loading as well as the corresponding fatigue damage.

II. DOUBLE ACTION SHOCK ABSORBERS

1. The Principles of Double Action Shock Absorbers and Typical Load/Travel Curves

Fig.1 is a schematic diagram of common double action shock absorbers. These shock absorbers have two gas chambers. The arrangement of the initial gas chamber at the top end and the normal oil-gas shock absorber arrangement are similar. The second gas chamber is inside the piston rod at the bottom end of the floating piston. The second gas chamber's charging pressure is relatively high in order to guarantee that the aircraft will run on rough runway surfaces. When the ground surface impact loading reaches a certain numerical value, it goes into operation. Because of this, the peak loading values go down for aircraft going over small bumps and depressions.
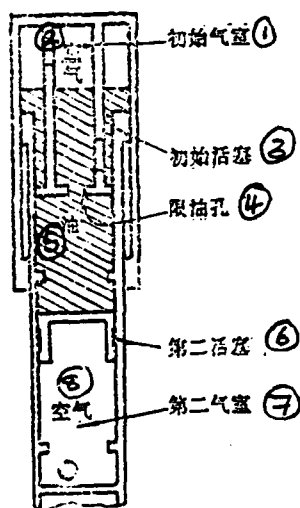

初始气室 ①
初始活塞 ③
限油孔 ④
第二活塞 ⑥
第二气室 ⑦

Fig.1 Double Action Shock Absorber 1. Initial Gas Chamber 2. Air
3. Initial Piston 4. Oil Limiter Aperture 5. Oil 6. Second Piston
7. Second Gas Chamber 8. Air

Fig. 2 is the load/travel static curve diagram for the standard short travel shock absorber, the long travel shock absorber, and the double action shock absorber. "AA'" is the short travel curve. This corresponds in Fig. 1 to the second piston being wedged in position and in an immobile status. "C" is the long travel curve. "AB" is the curve for the cooperative operation of the two gas chambers. The

20

intersection point "Q" of the two curves "A" and "B" is the break point at which the second gas chamber begins to operate.
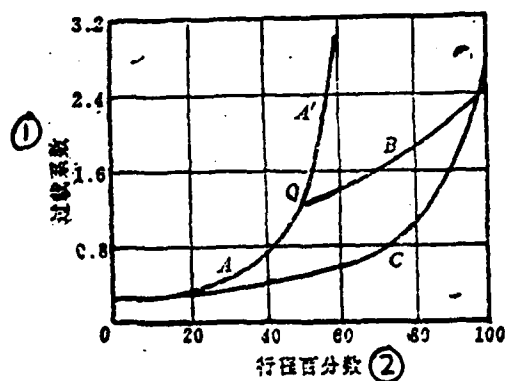

Fig.2 A Comparitive Diagram of Static Shock Absorber Curves 1. Overloading Coefficients 2. Travel Percentages
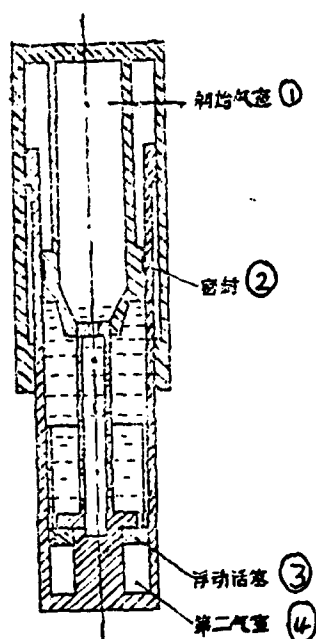

Fig.3 Schematic Diagram of an Improved Type of Double Action Shock Absorber 1. Initial Gas Chamber 2. Seal (unclear) 3. Floating Piston 4. Second Gas Chamber

On the basis of aircraft landing characteristics and the requirements of ground surface operations, with the foundation of the double action shock absorbers described above, further developments led to another type of improved double action shock absorber. See Fig. 3.

This type of shock absorber, besides possessing excellent performance characteristics on rough airfields, also requires the initial gas chamber and the second gas chamber point of operational intersection "Q" (See Fig.2) to have a vertical segment "EH" in which the travel stays equal and the load changes as shown in Fig.4. In terms of the structural arrangement, in order to guarantee this vertical section, at the top end of the floating piston there is a special arrangement for an extension section (See Fig.3). After the initial piston covers a section of the travel, the top of the extension section of the floating piston is used to mechanically push up against the bottom end surface of the outside tube rod piston, strongly limiting the compression of the second gas chamber. This causes the second gas chamber to begin operating.

The principal special features of a new type of double action shock absorbers are as shown below:

(1) As concerns the selection of the straight linear section "EM" as the appropriate locaiton, this guarantees that, when there are ground surface impacts, the shock absorbers will have enough reserve travel in order to achieve excellent performance characteristics on rough runway surfaces.

(2) In situations where aircraft have differing stationary loadings, the compression of the shock absorbers does not vary. This is advantageous for the ground support of the aircraft.

(3) Due to the fact that, after the take off run of the nose and main gear, the amount of the shock absorber compression is maintained basically unchanging, the angle of attack of the aircraft take off does not change, and this reduces the length of the aircraft take off run.

(4) Due to the fact that, when the left and right take off and landing gear shock absorbers run over the ground surface, the amount of compression remains basically unchanged, one avoids the problem of sideward sliding motion of outward slanted rod type main gear and reduces wear damage to tires.
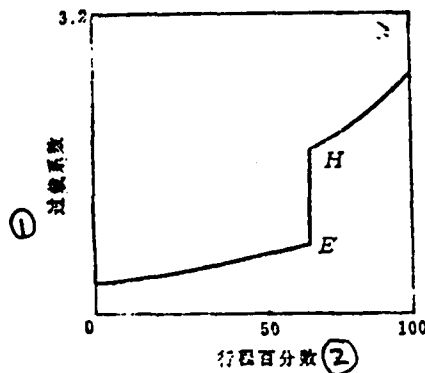

Fig.4 Graph of Static Curves for the Improved Type of Double Action Shock Absorbers 1. Load Coefficients 2. Travel Percentages

2. An Analysis of Static Characteristics of Double Action Shock Absorbers

(1) Dynamic Analysis Model

As far as whether or not the design of double action shock absorbers meets the requirements for adequate aircraft ground surface operating characteristics in such areas as landing impact, take off and landing runs, sudden braking, and so on, it is necessary to go into the calculations for a analysis of the dynamic effects in an aircraft simulation. From this, one can obtain the best parameters for the design of shock absorbers.

In Fig.5, we see presented the arrangement for equivalent masses and elasticity damping devices. These are used in analysis calculations of the dynamic influences or effects in double action shock absorbers. During the calculations, one ought to consider the non-linear tire and shock absorber gas spring, hydraulic damping, and the two types of effect models for aircraft structural rigidity and flexibility.
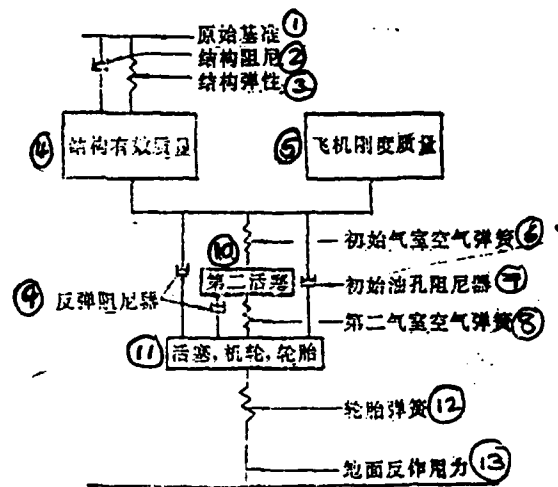
23

Fig.5 A Graphic Model of Take Off and Landing Gear and Aircraft
Structural Systems 1. Initial Basis 2. Structural Damping 3.
Structural Elasticity 4. Effective Structural Mass 5. Aircraft
Rigidity Mass · 6. Initial Gas Chamber Gas Spring 7. Initial Oil
Aperture Damping Device 8. Second Gas Chamber Gas Spring 9.
Resilient Damping Devices 10. Second Piston 11. Pistons, Wheels,
Tires 12. Tire Spring 13. Ground Surface Counter Force

In going through a dynamic analysis of the complete system, one
gets the relationships of the changes in load/travel when shock
absorbers are in operation.

(2) Slowly Going Over Long Wavelength Runway Surface Bumps

When aircraft are rolling in take off or landing runs, and they
slowly go over runway surface long wavelength bumps and depressions,

24

due to the fact that the speed of shock absorber compression is small, the speed at which hydraulic fluid inside the shock absorber flows through the small apertures is not great. The damping forces are relatively small and they act the same way as normal shock absorbers. The double action shock absorbers operate in accordance with curve "AB" (See Fig.2). Due to the fact that, after the loading from stopping the aircraft, the curve "AB" flattens out, its peak values of loading when crossing bumps on the runway surface are minimal.

Fig. 6 gives the travel and energy comparisons for three types of shock absorbers. Within the range of 1.0~2.0 units of overload increase, the travel and corresponding energy absorbtion for double action shock absorbers as compared to the other two model types are very much greater (See as shown in the Fig.6 by the shaded lines).
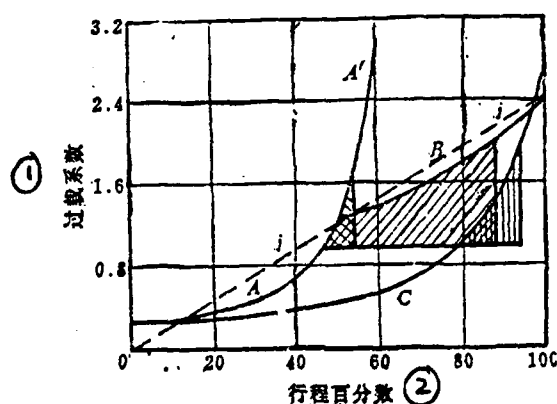
11

Fig.6   A Comparison of Shock Absorber Travel and Energies Going Over Runway Surface Bumps   1. Overload Coefficients   2. Travel Percentages

Table 1 supplies experimental data with which it is possible to quantitatively see the advantages of double action shock absorbers for use on rough runway surfaces.

① 项目 ② 增量 ③ 减震器 形式	④ 常规式	⑤ 双气室	⑥ 常规长行程式
⑦ 曲 线	AA'	AB	C
⑧ 行程增量	8.4%	41.6%	16.0%
⑨ 行程增量比	1.0	5.0	1.9
⑩ 能量增量	3.8	23.7	7.2
⑪ 能量增量比	1.0	6.2	1.9

Table 1 Experimental Data on the Properties of Three Types of Shock Absorbers 1. Item 2. Amount of Increase 3. Type of Shock Absorber 4. Standard Type 5. Double Action 6. Standard Long Travel Type 7. Curve 8. Amount of Increase in Travel 9. Ratio of Increase in Travel 10. Increase in Energy 11. Ratio of Increase in the Amount of Energy

From Table 1 it is possible to see that the travel of double action shock absorbers and the amount of increase in energy absorbtion are respectively 5 times and 6.2 times those of standard types. Moreover, as far as the ability to go over small bumps on runway surfaces is concerned, the former show values approximately 2.5 times those of the latter.

(3) Rapid Passage Over High Amplitude, Short Wavelength, Continuous Bumps

As far as the period of an aircraft's high speed take off and landing runs is concerned, when aircraft go over high amplitude, short wavelength, continuous bumps, tires are suddenly compressed. Their accumulated energies quickly come out as high pulse load, forcing the shock absorbers to quickly compress. The loading is quickly transfered over to the non-linear component of the shock absorber--the hydraulic fluid. Hydrualic fluids are not compressible. They are forced to flow at high speed through small apertures, forming very

large damping loads. Their values can be very large, reaching even to the point where they lead to overloading of the take off and landing gear. It is easy to ignore this point.

The impact loading on double action shock absorbers making a high speed traverse of bumps on runway surfaces is controlled by the second gas chamber. When the impact loads exceed a certain fixed value, the second gas chamber begins to operate. It is compressed and the hydraulic fluid is able to relatively slowly flow through the small apertures, entering into the upper cavity (See Fig.1). The reduction of hydraulic damping is very, very great. Because of this, it is possible for the artificial control of the shock absorbers, basically, to still operate along the curve "AB" (See Fig.2), lowering the peak ground surface loading values during take off and landing runs.

(4) Resilience Damping and Compression from Aircraft Stops Compared

During high speed take off and landing runs, after aircraft spring up or their wheels go over obstacles on the runway surface, the tire and shock absorber loads are reduced. The second piston should be fully extended in preparation for receiving the next impact. However, from dynamic analysis it is demonstrated that, at this time, the initial piston and the second piston both must have resilience or counterelastic control over bumps. This is advantageous for aircraft rolling rapidly in take off and landing runs over continuous large amplitude bumps on runway surfaces.

As far as ground surface take off and landing runs going over bumps is concerned, the size of the ability of double action shock absorbers to reduce loading and their compression ratios from aircraft stops are greatly related to their selection. Generally, they control approximately 50-60% in order to guarantee adequate reserve travel for crossing bumps. Their load/travel curve is even close to the linear spring curve "JJ". They are capable of reaching optimum increases in the amount of travel (See Fig.7). Moreover, the general run of long travel shock absorbers, due to the fact that their curves cross under the others (See Fig.2) have compression ratios from the stopping of the aircraft of approximately 80%. This is not a good characteristic for crossing runway bumps.
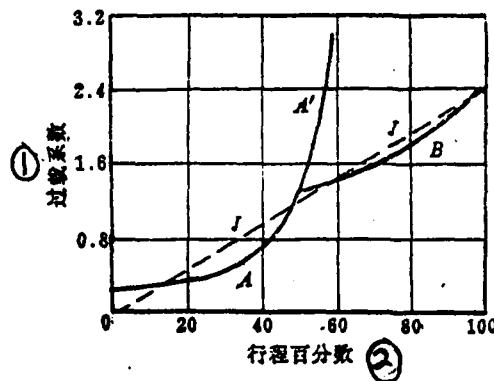
27

Fig.7 Equivalent Linear Spring for Double Action Shock Absorbers 1. Overload Coefficients 2. Travel Percentage

(5) Landing Impact Characteristics

As far as the standard type of shock absorber is concerned, aircraft design makes use of landings at less than sinking speed. This assumes that the corresponding design for landing overload coefficients is 1.5. The load/travel curve is as shown in curve "D" in Fig.8.

If one takes the sinking speed and increases it by 50%, then, these shock absorbers should possess 2.25 times the energy absorbtion capability. At such a time, the corresponding load/travel curve is "E". Its load value increases approximately one fold.

If double action shock absorbers are selected for use, in the same sort of design, they will be used at less than sinking speed. Due to the fact that the load in curve "D" (See Fig.8) is slightly more than the peak pressure load of the second gas chamber, the second piston will show a small amount of downward movement. The load/travel curve is the curve "F" (See Fig.9). The shock absorber load drops slightly. If one takes the sinking speed and increases it 50%, the shock absorber quickly compresses, causing the oil pressure at the top end of the second piston to quickly increase. This forces the second
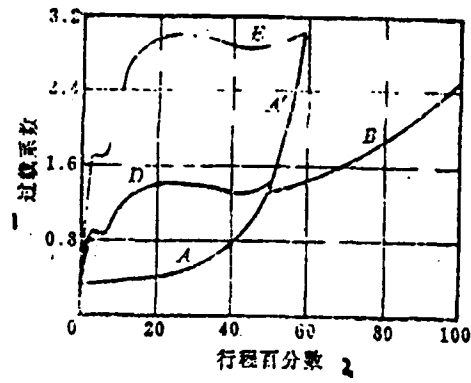
12

Fig.8: Load travel curve.
1-Overload coefficient 2-travel percentage

gas chamber into operation. The speed of the flow of the hydraulic
fluid through the small apertures slows. This lowers the hydraulic
fluid damping stength. Finally, the shock absorber operates along the
curve "H" shown in Fig. 9. However, due to the fact that the sinking
speed has already been increased 50%, the "H" curve is obviously above
the "F" curve (Theoretically, the bottom section area of the "H" curve
is equal to the bottom section area of the "E" curve).

The "G" curve shown in Fig.9 is the upper limit of the first half
load travel curve for double action shock absorbers. Due to the fact
that, at the time of landing impact, the second gas chamber is in
operation, it follows that the "F" curve is certainly below the "G"
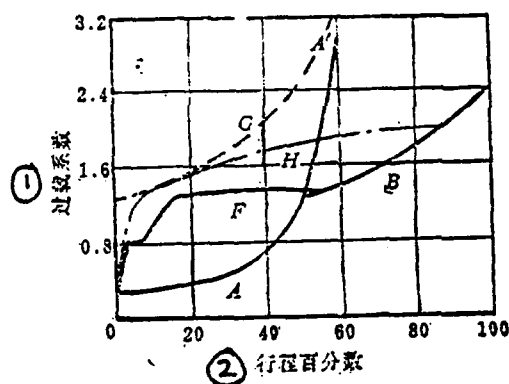curve.

Fig.9 Double Action Shock Absorber Descent Shock Test Curve 1.
Overload Coefficients 2. Travel Percentages

From Fig. 9 one can see that, due to the fact that the second gas
chamber is in operation, it is possible to lower the overload on the
shock absorbers approximately 1/3.

(6) As far as the load accepting capability of high sinking
speeds is concerned, it is possible to make appropriate use of them in
short take offs and landings.

Double action shock absorbers can greatly raise the load
accepting capabilities at landing sinking speeds. Because of this, it
is possible to land at a relatively short airfield or one at which the
runway has been damaged and there is only a section left (See Fig.10).
This type of landing (called a hard landing) is not the same as a
normal smooth, floating landing. In this landing, one uses a
relatively large angle of slope to enter the airfield in order to make
a landing in such a configuration that there is a minimal section of
level flight or no section of level flight at all. This is done in
order to obtain the optimum touch down point, reducing the distance
from the landing point to the end of the runway (for normal landings
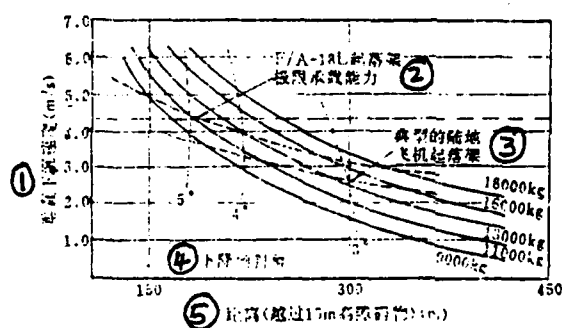500m-700m) and improving landing characteristics.

Fig.10 The Curve for Touch Down Point Distances Versus Changes in

Sinking Speed 1. Perpendicular Sinking Speed (m/s) 2. Basic Load

Accepting Capability of F/A-18L Take Off and Landing Gear 3. Aircraft

Take Off and Landing Gear in Classical Landing 4. Lowered Angle of

Slope 5. Distance (Going Over Obstacles 15m High (unclear)) (m)

Besides this, in actual use, at medium and high sinking speeds,

the load accepting capabilities of shock absorbers are capable of

being used on runway surfaces with relatively high degrees of

roughness.

31

Fig.11 is the U.S. C-130E aircraft. It shows the relationship between load accepting capabilities at recommended sinking speeds and the degree of roughness of runway surfaces. When one is using the normal sinking speed for designs, which is 3m/s, the corresponding ground surface bump amplitude is 254mm. When one is using the maximum sinking speed of 5.2m/s, it is necessary that the runway surface be completely smooth.

(7) Reduced Braking Leading to Nose Wheel Overload

When aircraft are making their take off and landing runs on the ground surface, and they make sudden use of their brakes, the aircraft goes down toward the nose wheel. This creates a very large vertical sinking speed compression of the shock absorbers. The standard type of shock absorbers are capable of producing very large overloads. However, double action shock absorbers only produce very small overloads. As is shown in Fig.12, the peak load values of the former lie at point "C", and, compared to the peak load values of the latter, at point "D", are much higher.
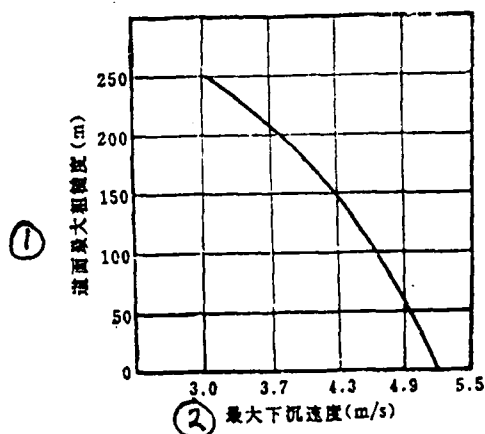
13

Fig.11 The Curve Relating Double Action Shock Absorber Load Accepting Capabilities and the Degree of Roughness of Runway Surfaces 1. Macimum Degree of Runway Surface Roughness (m) 2. Maximum Sinking Speed (m/s)
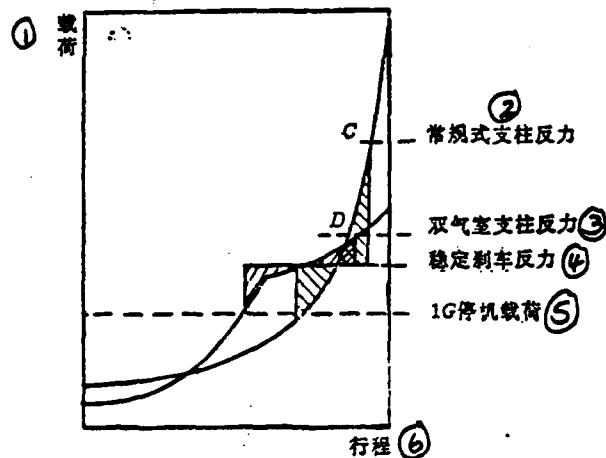
Fig.12 The Use of Double Action Shock Absorbers in the Reduction of
Braking Leading to Excessive Nose Wheel Loading 1. Load 2. Standard
Rod Counter Force 3. Double Action Rod Counter Force 4. Stable
Braking Counter Force 5. 1G Stopping Load 6. Travel

III. DOUBLE ACTION SHOCK ABSORBER PARAMETER SELECTION

1. Initial Estimate of Load Coefficient

From reference (1) it is possible to know that

$$\frac{V^2}{2g} = N(0.7S_p + nS_s + 0.47T)$$

In this equation N--Load Coefficient

0.7--The assumed rod efficiency coefficient

S_p--Initial gas chamber travel

T--Tire travel

n--Second gas chamber efficiency coefficient
(approximately 60%)

S_s--Second gas chamber travel

It is then possible to calculate the load coefficient N. The initial
estimate can be used in the equation below to calculate the load
coefficient N

$$\frac{V^2}{2g} = N(0.7S + 0.47T)$$

In this equation: S--Overall travel

For the parameters concerned the recommended ranges to use can be
seen in Table 2.

	① 双气室	② 常规式
③ 全压缩载荷/ 停机载荷	主起落架2; 前起落架3 ④	主起落架 3 ⑤ 前起落架4~5
全伸展支柱载荷/ ⑥ 停机载荷	1/3	1/4
伡机压缩行程/ ⑦ 总行程	0.5—0.6	0.5~0.6
⑧ 第二气室开始工作	粗糙机场取1.2g ⑩	
⑨ 载荷/行程转折点	考虑疲劳和主跑道面 取0.8g ⑪	

⑫ ①第二气室开始工作的转折点, 用于粗糙机场 时 取用
1.2g以防止飞机正常地面滑行时第二气室间断工作.

Table 2 Ranges Recommended for Use as Parameters 1. Double Action
2. Standard Type 3. Full Compression Load/Aircraft Stop Loading 4.
Main Take Off and Landing Gear 2; Front Take Off and Landing Gear 3
5. Main Take Off and Landing Gear 3   Forward Take Off and Landing
Gear 4-5 6. Full Extension Rod Load/Aircraft Stop Load 7. Second Gas
Chamber Begins to Operate 9. Load/Travel Break Point 10. Roughness
of the Airfield Taken as 1.2G (1) 11. Consideration Given to Fatigue
and Main Runway Surface Taken as 0.8g. 12. (1) As far as the break
point at which the second gas chamber begins to operate is concerned,
when one is using rough airfields, one selects for use the value 1.2g
in order to prevent the second gas chamber operation breaking in
during the normal ground surface run time of the aircraft.

2. Selection of Important Parameters for Standard Type Double Action Shock Absorbers

(1) Parameters that are already known or assumed (from the layout of the aircraft or selected for a standard aircraft)

Rod full compression load; Rod aircraft stop load; Rod full extension load; Curve breakpoint load; Rod travel during aircraft stop; Overall rod travel (determined on the basis of overload coefficient); Shock absorber aircraft stop pressure; Shock absorber piston surface (A).

(2) Calcualtion of Shock Absorber Charging Coefficient

Full extension pressure

$$p_e = \frac{P_e}{A}$$

In this equation P_e--Rod full extension load (already known).

Initial chamber volume during aircraft stops

$$V_s = V_e - (S_s \times A)$$

In this equation S_s--Aircraft stop travel (already known).

Initial chamber volume for complete extension   14

$$V_e = \frac{p_s V_s}{P_e}$$

In this equation p_s--Shock absorber pressure for aircraft stops (already known).

Initial chamber pressure for the start of second gas chamber operation

$$p_{1s} = \frac{1.2 \times p_s}{A}$$

Initial chamber air volume for the start of second gas chamber operation

$$V_{1s} = \frac{p_e V_e}{P_{1s}}$$

Compressed to the initial chamber travel V_{1s}

$$S_{1s} = \frac{V_e - V_{1s}}{A}$$

Initial chamber full compression pressure

$$p_c = \frac{P_c}{A}$$

In this equation P_c--Rod full compression load (already known).

Initial chamber full compression volume

$$V_c = \frac{p_e V_e}{P_c}$$

If one makes δV_c the change in total gas chamber volume from the beginning of second gas chamber operation until full rod compression is reached, then

$$\delta V_c = (S_c - S_{1s}) \times A$$

In this equation S_c is the overall rod travel (already known).

$$\delta V_c - V_c = V_{2s} - V_{2s} \qquad (1)$$

In this equation V_{2s} is the second gas chamber volume at full extension; V_{2c} is the second gas chamber volume at full compression; $V_{2s} - V_{2c}$ is the change in the amount of the volume when the second gas chamber goes from extension to full compression.

$$p_{2s}V_{2s} = p_{2c}V_{2c} \qquad (2)$$

$$p_{2s} = p_{1s} = p_{2e} \qquad (3)$$

$$p_{2c} = p_c \qquad (4)$$

In these equations p_{2s} is the initial second gas chamber pressure; p_{2c} is the second gas chamber pressure at full compression; p_{2e} is the second gas chamber pressure at full extension.

From equation (1), equation (2), equation (3), and equation (4), it is possible to solve for V_{2s} and V_{2c}.

(3) Shock Absorber Load/Travel Curve

  (a) Before the Breakpoint

$$V_2 = V_e - S_{1,i} \times A \qquad P_2 = p_2 \times A$$

$$p_2 = \frac{p_e V_e}{V_2} = \frac{p_e V_e}{V_e - (S_{1,i} \times A)} \qquad (5)$$

In these equations $S_{i,i}$ is the shock absorber travel before the breakpoint.

From equation (5), it is possible to solve for a section of the shock absorber curve before the breakpoint.

  (b) After the Breakpoint

$$V_2 = (V_{2e} + V_{1s}) - (S_{2,i} \times A)$$

$$p_2 = \frac{p_{1s}(V_{2e} + V_{1s})}{V_2} =$$

$$\frac{p_{1s}(V_{2e} + V_{1s})}{(V_{2e} + V_{1s}) - (S_{2,i} \times A)} \qquad (6)$$

$$P_2 = p_2 \times A$$

In these equations $S_{2,i}$ is the shock absorber travel after the breakpoint of the curve.

From equation (6), it is possible to solve for a section of the shock absorber curve after the breakpoint.

  (c) The combining of the two sections of the curve before and after the breakpoint gives one the solution for the double action shock absorber load/travel curve.

IV. RUNWAY SURFACE ROUGHNESS

As far as the quality of double action shock absorber characteristics is concerned, it is necessary to carry out experimental verifications of them through simulations of aircraft ground surface runs and dynamic impacts. The dynamic analysis requires the introduction of a set of data which are able to simulate standard runway surface roughness. Reference (1) provides specific data and equations for the expression of them to fit the three types of unprepared, semi-prepared, and concrete runways.

Reference (2), on the basis of the the U.S. theater of operations airfield deployment, provides suggested standards for airfield roughness. These can be divided into four catagories of airfield.

From Fig.13 and Fig.14, it is possible to see that the numerical values suggested by reference (2) are slightly higher than reference (1), causing it to be on the safe side. In the situation in which our country finds itself, with no strict standards of roughness, it is possible for us to consult these references.   15
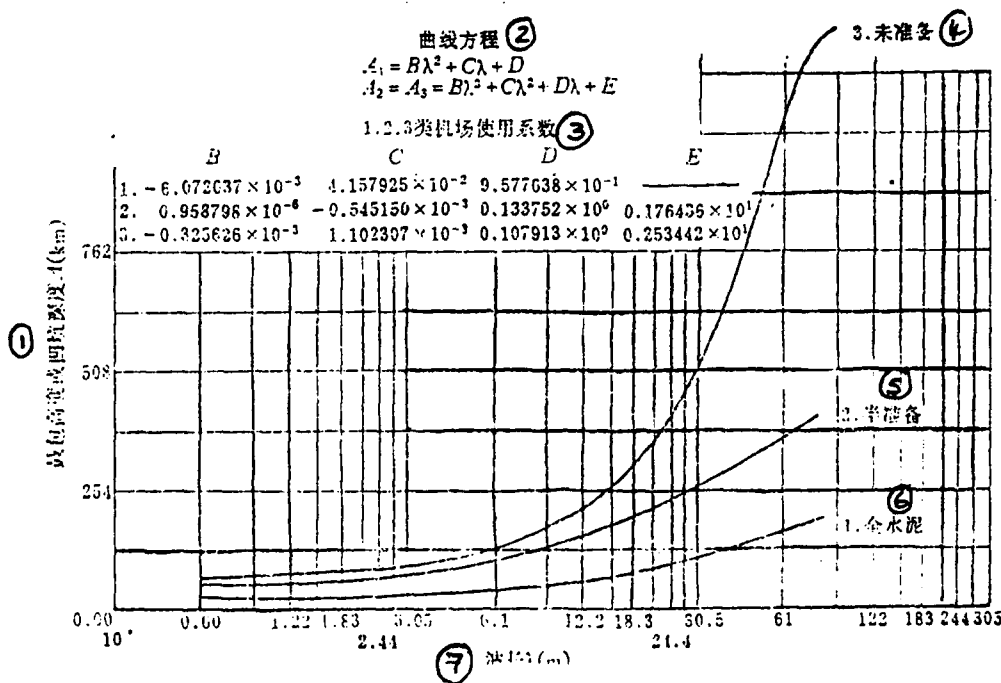

Fig.13 Graph of the Relationship Between the Amplitude of Non-Continuous Undulations and Wavelength for Semi-Prepared, Unprepared, and Concrete Runway Surfaces   1. Height of Rise or Depth of Depression A (km)   2. Curve Equations   3. Coefficients for the Use of Types 1,2,and 3 Airfields   4. Unprepared   5. Semi-Prepared   6. Full Concrete   7. Wavelength λ (m)
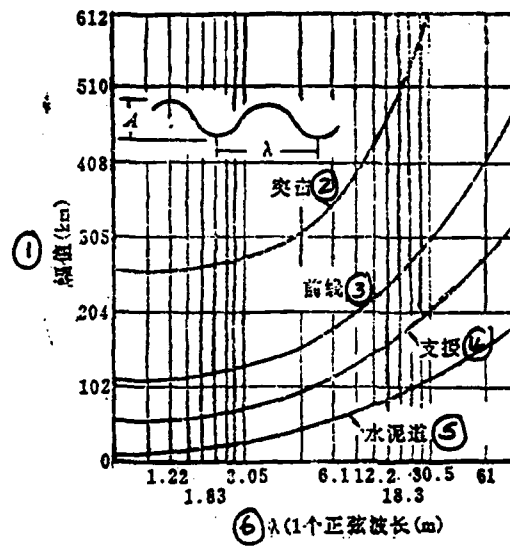
Fig.14 Suggested Airfield Roughness Standards   1.   Amplitude Value
(unclear) (km) 2. Breakthrough 3. Front Line 4. Support 5.
Concrete Runway 6.   λ (1 Sinusoidal Wavelength (m))

V. MISCELLANEOUS

As far as the use of shock absorbers on rough airfields is
concerned, there are still two types of deployment plan.

1. The Selection for Use of Long Travel Shock Absorbers With Load
Release Spring Valves Fitted to the Shock Absorber Piston Rod Fluid
Needles (See Fig.15)
At times when aircraft passing over ground surface bumps give rise to
sudden changes in load, the high pressure fluid chamber fluid pressure
compression load discharge valve spring causes a portion of the
hydraulic fluid to flow through apertures in fluid limiter needle
rods. It flows along the overload fluid release path and into the
upper cavity, preventing overload.

2. The Selection for Use of Double Action Shock Absorbers in
Conjunction with Special Fluid Limiter Needle Rods (See Fig.16)
In the design of the take off and landing gear of the F/A-18L, these
acheived obvious results. The oil limiter needle rods, in locations   16
corresponding to aircraft stops, make use of relatively small areas in
order to obtain relatively large fluid apertures, reducing the damping
going over bumps. In design, the configuration of the oil limiter

needle rods should be studied in particular. Reference (3) introduces the design for the oil limiter needle rod. The Northrop Company has selected 30 models out of which to choose the best in order to get the appropriate shock absorber characteristics.
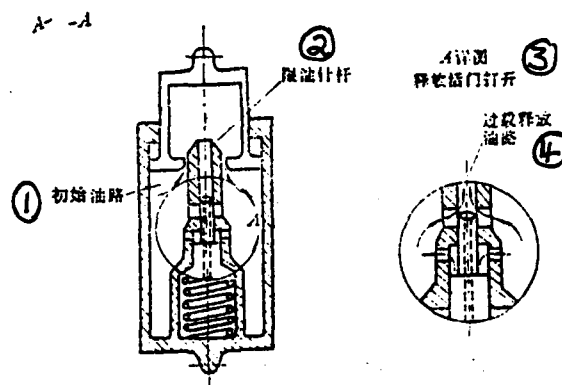

Fig.15 Illustrative Diagram of Oil Limiter Needle Rod System 1. Initial Oil Path 2. Oil Limiter Needle Rod 3. Diagram of Open "A" Type Release Valve 4. Oil Overload Release Path
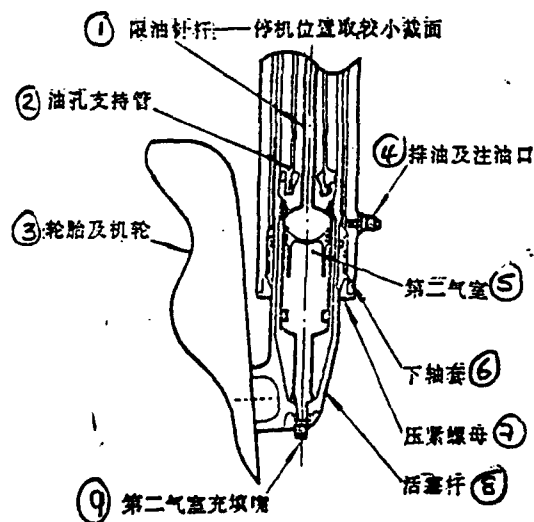

Fig.16 Double Action Shock Absorbers Used in Conjunction With Special Oil of Fluid Limiter Needle Rods 1. Oil or Fluid Limiter Needle Rod -- Takes Relatively Small Cross Section in Aircraft Stop Position 2. Fluid Aperture Support Tube 3. Tires and Wheels 4. Fluid Insert and Withdrawal Port 5. Second Gas Chamber 6. Lower Axle Sleeve 7. Tightening Nut (unclear) 8. Piston Rod 9. Second Gas Chamber Charging Port

REFERENCES

(1) MIL-A-8862(USAF).

(2) Williams, W. W. ,Williams, G. K. and
    Gahard, W. C. J. ,Soft and Rough Field
    Landing Gear, SAE 650844 (1965).

(3) A Fighter Landing Gear for the 1980's
    AGARD-CP-336, (1980).

SEMI-PREPARED AIRFIELD AND DESIGN OF DOUBLE -ACTION SHOCK ABSORBER

Gao Zhejun

(*Huaxi Institute of Mechanical Automation*)

A88·29255

Abstract

As to design of landing gear, the paper points out that the stroke of a conventional single-action shock absorber is too short to absorb the impact energy induced by taxing of an airplane on rough runways. They will, therefore, transmit very large loads on to joints and supporting structures of the landing gear and lead to abrupt damage or short fatigue life.

In order to control the impact loads, long stroke double-action shock absorbers have been developed to absorb the impact energy due to landing or takng-off on rough airfields, the peak value of impact loads being *noticeablly* reduced.

Futhermore, the paper discusses the structural type of the landing gears suitable for rough fields, in particular the design conception and characteristics of double-action shock absorbers and compares them with conventional landing gears in many respects.

THE ANALYSIS FOR DYNAMIC RESPONSE DURING AIRPLANE TAXIING

Liu Ruishen

SUMMARY This article, setting out from standards for the uneveness of airfield runways, is based on the concept of power spectra. It introduces basic methods for measuring random variables from the uneveness of airfield runways. It drafts curves for the power spectra of uneven runways and carries out a preliminary analysis of the dynamic effects in aircraft ground surface taxiing.

I. INTRODUCTION

The problem of dynamic loading in ground surface taxiing is one of random vibration phenomena.

Random vibrations from the uneveness of airfield runways severely effect take off and landing gear as well as aircraft structural strength. Take off and landing gear must cope successfully with any energies stemming from this and have the capability of preventing fatigue. Fuselage structures should also have sufficient fatigue life. If one calculates a year of aircraft use as 400 hours, then, it will taxi approximately 30,000 km and will experience 50 million cycles of random stress in taxiing. The life of civil aircraft is 20 years. In this time, it is possible to reach a billion cycles of stress. Because of this, the damage produced is an important component (1) in overall aircraft structural damage. Besides this, vibrations from the uneveness of runways can also lead to deterioration of the cabin environment and a drop in the visibility of the instrument panel, preventing pilots from accurately controlling the capabilities of the aircraft and reducing the reliability of aircraft landing functions.

There are two basic methods of conducting an analysis of dynamic effects in ground surface taxiing, that is, the frequency domain of power spectra method and the time domain determination method. The power spectrum method involves taking the random excitations and expressing them by forming power spectra. In working out the stability of the random or stochastic process, given such assumptions as the normalization of damping and the linearization of rigidity, one sets out the differential equations of motion. In frequency domains, one solves for the various effect parameters, taking power spectrum

curves to show the uneveness of runways and deduce the random load
spectra for taxiing. One then carries out a structural life analysis
for the take off and landing gear. In the case of large and medium
types of aircraft, the air-ground-air cycle is the principal cause of
fatigue damage. Moreover, the random loads of taxiing also form a
component part of the peak and valley values of the ground-air-ground
cycle.

Accurate methods are capable of overcoming the various degrees of
inappropriateness and shortcomings introduced in the power spectrum
method by the assumptions of stability, equivalent damping, and linear
rigidity. Moreover, it takes the uneveness of runways and makes it
into an implicit function for substitution. Precision methods make
use of rigorous methods of analysis to solve for the
motion equations for the free modality of aircraft taxi movements,
including non-linear systems. It is appropriate for use in
calculating peak value effects for ground surface movements (for
example, landing shock, taxiing, turning, and taking off). Due to the
fact that each calculation is only appropriate to a particular case,
it is necessary to carry out large scale sampling. Only then is it
possible to obtain statistical results. Obviously, compared to the
power spectrum method, the number of calculations must be much
greater.

II. STANDARDS FOR RUNWAY UNEVENESS

In order to carry out the setting up of runway power spectrum
curves, it is necessary to carry out actual measurments of the degree
of uneveness of various types of airfield runways.

In the 1950s, the U.S. made relatively early use of methods from
the manual arts, making use of the three basic types of measurement
devices--the level, the tape measure, and the aiming stake--to gather
data on the uneveness of airfield runways (2,3).   19

The current measurement methods already make use of
oscilloscopes, recording paper, magnetic tape recording, and other
automatic recording equipment to record and process data. It is
possible to gather large amounts of data on the uneveness of runways
quickly.

The empirical formula for making up power spectrum density curves from the results of actual measurements is

$$\Phi(\Omega) = C/\Omega^A \qquad \qquad (1)$$

In this equation, Ω is the spatial frequency. Moreover, $\Omega = \omega/v$; ω is the time frequency; v is the taxi speed; A and C are the coefficients representing the runway characteristics.

From $\lg \Phi(\overline{\Omega}) = \lg C - A \lg \Omega$, it is possible to see that, on logrithmic coordinates, it is a true linear relationship. National military regulations provide three types of airfield runway power spectrum density curves to act as the basis for the ground surface load spectrum taxi loading. These were put together on the basis of the results of large amounts of empirical measurement data. Actual application demonstrates that this set of curves is relatively reliable. In order, from theory, to verify equation (1), it is still necessary to carry out the corresponding calculations and analysis.

1. Statistical Characteristics of Stochastic Processes

Power spectrum analysis methods are one method for the analysis of stochastic processes. On the basis of generalized harmonic theory, for a power spectrum analysis of a stochasitc process, it is necessary to satisfy the assumptions of stable, universally applicable, and Gaussian distributions.

If one measures the vertical displacement of an aircraft taxiing on the same runway, the vertical displacements measured for different time periods are respectively $x_1(t)$, $x_2(t)...x_k(t)(k=1,2,...n)$. The time relationship curves are all different from each other. This is due to influences which are impacted on by several random factors. For example, the uneveness of the runway; the taxi configuration, and the speed; the wind direction and the wind speed; the skill of the pilot, and so on. The same aircraft, under the same conditions, will not have the same wave form for its vertical displacements each time it goes down the runway.

Among statistical quantities which are capable of reflecting the

basic characteristics of random variables, there are the geometric mean (mathematical expectation), mean square value, root mean square value and square difference, as well as other similar quantities. According to the description of the time domain, their definitions are respectively as follows.

The geometric mean value is

$$E[x(t)]=\mu_x=\lim\frac{1}{T}\int_{-T/2}^{T/2}x(t)dt$$

The mean square value is

$$E[x^2(t)]=\psi_x^2=\int_{-T/2}^{T/2}x^2(t)dt$$

The square difference is

$$E[\{x(t)-\mu_x\}^2]=\sigma_x^2$$
$$=\lim\frac{1}{T}\int_{T/2}^{T/2}(x-\mu_x)^2dx$$

One can obtain the relational formula

$$\sigma_x^2=\psi_x^2-\mu_x^2$$

or

$$\psi_x^2=\sigma_x^2+\mu_x^2$$

This shows that the mean square value displays the strength of the random variable. One can see that it is the sum of the static component which does not change with time and the dynamic component which changes with time. According to the characteristics of a normal probability distribution, it is possible to select a characteristic curve for a certain parameter (such as overload) as it varies through time on a runway of the same type. The normal probability density function is capable, from the mean value μ_x and standard deviation

46

σ_x, of being expressed as

$$P(x) = \frac{1}{\sigma_x \sqrt{2\pi}} exp \left[-\frac{(x-\mu_x)^2}{2\sigma_x^2} \right]$$

(2)

Because of this, it is possible to obtain statistical parameters for the random variable of runway roughness.

In considering random vibrations, one important statistical quantity is still necessary, that is, an autocorrelation function. This is information or data on the dependent relationship connecting the value of a random variable at a certain instant and the value of this variable at another instant. Its definition is

$$R_x(\tau) = \lim_{T \to \infty} \int_{-T/2}^{T/2} x(t)x(t+\tau)dt$$

(3)

In this equation, τ is the time interval variable.

If there is no relationship between the time t and the geometric mean value $, \mu_x(t)$ and autocorrelation function $R_x(\tau)$, then, the process is stable (steady state process). If the geometric statistical characteristics for multiple occurrence samplings (mean values for full scale populations and autocorrelation functions for full scale populations) and unit sampling statistical characteristics (average time values and autocorrelation functions for time) are respectively equivalent, then, this process is ergodic. Under ergodic condtions, it is possible to make independent use of a sample function in order to describe the given stochastic process. Moreover, it is not necessary to consider sampling the full population.

20

There are practical difficulties that exist with large scale samplings. As far as practical measurements to discover the roughness of airfield runways are concerned, although the data for several measurements of the same runway are not the same, their statistical characteristics (it is only necessary that the degree of wear on the runway not be too great) during short periods will not show any relatively large differences. It is possible to recognize that, in such a case, the situation is stable and ergodic unless this is negated by some obvious cause. This is the basic assumption in our carrying out of power spectrum analyses. Autocorrelation functions and power spectrum density functions are basically in line with each other. The former provide information on the nature of relevant random variables within the time domain. The latter provide similar information for frequency domains. If one is speaking of ergodic processes, it is possible to mutually interchange autocorrelation functions and power spectrum density functions.

We choose the autocorrelation function of the sample selection function x(t) to be

$$R_x(\tau) = lim \int_{-T/2}^{T/2} x(t) x(t+\tau) dt$$

In this case, its power spectrum density function is the Fourier (3) transform of $R_x(\tau)$. That is,

$$S_x(\omega) = \int_{-\infty}^{\infty} R_x(\tau) e^{-i\omega\tau} d\tau$$

The autocorrelation function is also capable of being gotten from the Fourier inverse transform, that is

$$R_x(\tau) = \frac{1}{2\pi} \int_{-\infty}^{\infty} S_x(\omega) e^{i\omega\tau} d\omega$$

If $\tau = 0$, then

$$R_x(0) = \lim_{T \to \infty} \frac{1}{T} \int_{-T/2}^{T/2} x^2(t)dt$$

and

$$R_x(0) = \frac{1}{2\pi} \int_{-\infty}^{\infty} S_x(\omega)d\omega$$

One can see that, within the whole frequency range, the integral of the power spectrum or the area under the power spectrum density function curve is the mean square value of the runway unevenness. That is,

$$\psi_x^2 = \int_{-\infty}^{\infty} S_x(\omega)d\omega$$

It is normally required that the mean square value must be controlled within a certain range. If not, then, the runway or taxiway should be repaired or redone (5).

2. Data Processing With Autocorrelation Functions

In using empirically measured data in drafting up autocorrelation functions, it is possible to use wave filter methods. Speaking in terms of load spectra or effect calculations, the significance of long waves is not great. It is possible to eliminate it through wave filtration. For 150m section of runway, at each 2 meters, one selects a point. Then, the mean value of the height displacement can be defined as being

$$y'(x) = \frac{1}{150} \sum_{k=-75}^{k=75} y(x+k\triangle x)$$

In this equation, k is the number of points.

This value is shown by the dotted line in Fig.1 (before wave filtering). The changes in the runway height along the mean value of the displacement form the shape in the Fig. after wave filtration. The results of the low frequency portion have been filtered out.
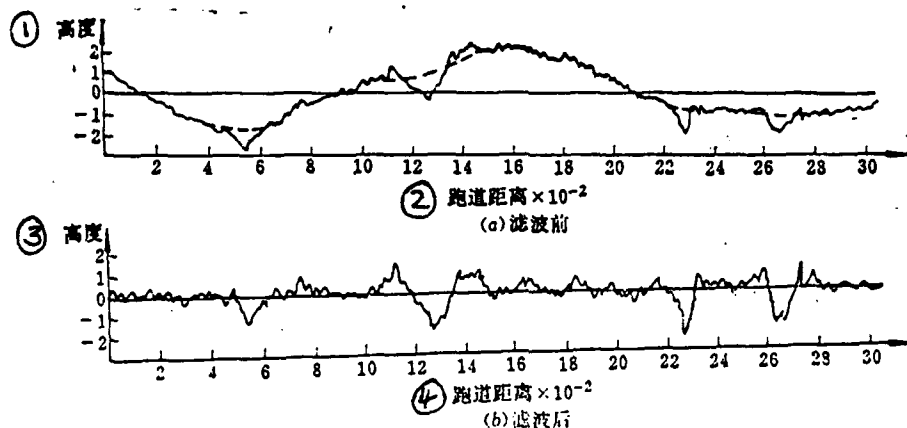

Fig.1 Diagram of Runway Height Before and After Wave Filtering 1. Height 2. Runway Distance x 10^{-2} (a) Before Wave Filtering 3. Height 4. Runway Distance x 10^{-2} (b) After Wave Filtering

Sample calculations from measurement data on a given runway are shown in Table 1.

21

① 点号 N	② 跑道距离x (m)	③ 剖面高度y (m)
1	0	−0.2156
2	0.6	−0.2301
3	1.2	−0.1984
4	1.8	−0.1871
5	2.4	−0.1676
6	3.0	−0.1624
7	3.6	−0.1527
⋮	⋮	⋮
67	39.6	0.0216
68	40.2	0.0167
69	40.8	0.0143
⋮	⋮	⋮
698	418.2	−0.0655
699	418.8	−0.0655
700	419.4	−0.0643
701	420.0	−0.0337

Table 1 Measurement Data on a Certain Runway 1. Point No. 2. Runway Distance 3. Cross Section Height 50

Choose the aircraft runway speed to be v = 160km/h. Choose the aircraft frequency range to be f = 0.5~35 Hz. The corresponding wavelengths are λ = 1.2~90m. According to information from the principles of selection, at half the interval between the shortest wavelengths, the interference which is taken out, entirely represents the indicated interference . Select the number reading period to be 0.6m. The runway measurement length is 420m. The number of measurement points is 701.

The autocorrelation function calculation formula is as shown below

$$R_r = \frac{1}{N-r} \sum_{n=0}^{N-r-1} Y_n \cdot Y_{n+r}$$

$$(r=0, 1, 2, \cdots m)$$

In this equation, N is the number of measured points, which is 701. n is chosen with a value such that n ≤ N. m is the number of uniform points dividing up the frequency range, which is 41. r is chosen with a value such that r ≤ m.

$$r=0 \quad R_r = \frac{1}{701}(y_0^2 + y_1^2 + y_2^2 + \cdots$$
$$+ y_{700}^2)$$

$$r=1 \quad R_r = \frac{1}{700}(y_0 \cdot y_1 + y_1 y_2 + y_2 y_3$$
$$+ \cdots + y_{699} y_{700})$$

$$r=2 \quad R_r = \frac{1}{699}(y_0 y_2 + y_1 y_3 + y_2 y_4$$
$$+ \cdots + y_{698} y_{700})$$

$$\vdots \qquad \qquad \vdots$$

$$r=41 \quad R_r = \frac{1}{660}(y_0 y_{41} + y_1 y_{42} +$$
$$y_2 y_{43} + \cdots + y_{660} y_{700})$$

As far as the results of this are concerned, it is possible to draw the autocorrelation function curve as it is shown in Fig.2.
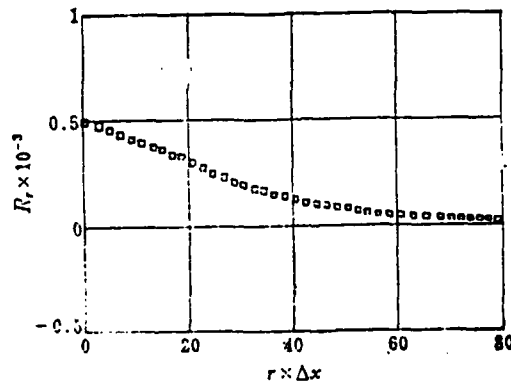
Fig.2 Autocorrelation Coefficients for Runway Height

3. Data Processing for Power Spectrum Density Function Curves

The method of making Fourier transformations from autocorrelation functions and calculating power spectrum density function curves belongs to the standard ones. As far as single-sided or unilateral power spectra are concerned

$$S_x(f) = 2\int_{-\infty}^{\infty} R_x(\tau)e^{-i2\pi f\tau}d\tau \quad (0 \leqslant f < \infty)$$
$$= 2\int_{-\infty}^{\infty} R_x(\tau) \cdot \cos2\pi f\tau d\tau$$

The above equations should provide discreteness. Due to the fact that the analytical process x(t) is a stable stochastic process, one assumes that the cut off frequency is f_c. Then, in the time aomain, for the time of sample selection x(t), according to the principles of sample selection, that is

$$f_e = \frac{1}{T_e} = \frac{1}{\Delta t} = 2f_c$$

The interval for which it is possible to choose samples is

$$\Delta t = \frac{1}{2f_c}$$

If one takes x(t)'s frequency variation range $(0, f_c)$, that is, $[0, \frac{1}{2\Delta t}]$ and divides it into m sections, then, the interval of sample selection for the frequency domain is

$$\Delta f = \frac{1}{m}\left(\frac{1}{2\Delta t}\right) = \frac{1}{2m \cdot \Delta t}$$

The frequency sample selection point is

$$f_i = k \cdot \Delta f = \frac{k}{2m \cdot \Delta t} \qquad (k = 0, 1, 2 \cdots$$
$$m - 1)$$

The sample selection period $\Delta \tau = \Delta t$; Moreover, selecting 2m time delay values, then

$$\tau = r \cdot \Delta \tau = r \cdot \Delta t \qquad (r = -m, \cdots -1,$$
$$0, 1, 2 \cdots m - 1)$$

Because of this, the unilateral power spectrum diffusion form or form of discreteness is

$$S_x(f) = 2\sum_{r=-m}^{m-1} R_x(r \cdot \Delta t) \cdot \cos(2\pi k \cdot \Delta f$$

$$\cdot r \Delta t) \cdot \Delta t$$

$$= 2 \cdot \Delta t \sum_{r=-m}^{m-1} R_x(r \cdot \Delta t) \cos\left(\frac{\pi k r}{m}\right)$$
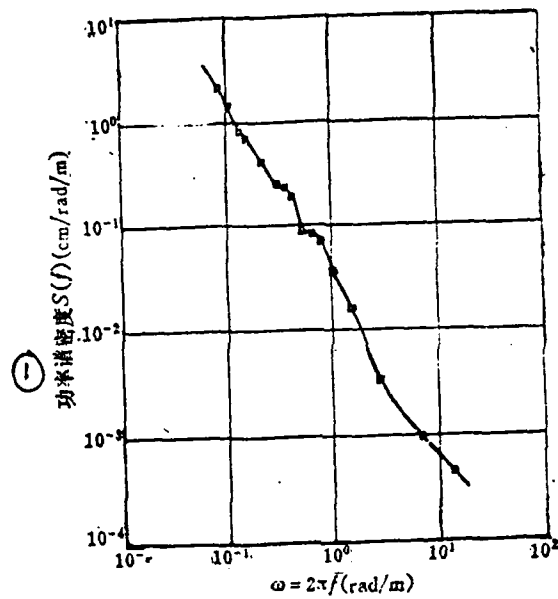
After considering boundary conditions, the final result is

Fig.3 Power Spectrum Curve Formed from an Inversion of R_r 1. Power spectrum density

$$S_x(f) = 2 \cdot \Delta t (R_x(0) + 2\sum_{r=1}^{m-1} R_x(r)$$

$$\cos\left(\frac{\pi k r}{m}\right) + R_x(m)(-1)^r)$$

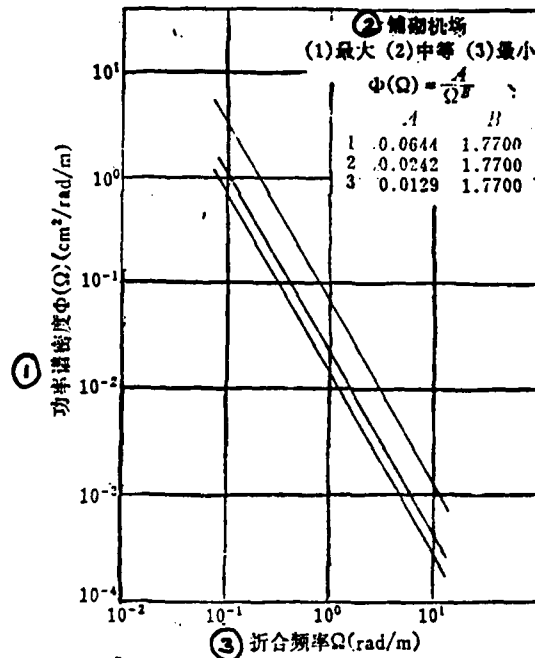$$(k=0, 1, 2, \cdots m-1) \qquad (4)$$

Fig.4 Power Spectrum Curves for Paved Runways 1. Power Spectrum Density 2. Paved Airfields (1) Largest (2) Medium (3) Smallest 3. Frequency Calculation

On the basis of Fig.2, one inverts it and forms the graph of $S_x(f)$ as shown in Fig.3.

The power spectrum density function curves for the three types of paved airfields as provided in National Defense Military Standard (GJB67.6-85) are shown in Fig.4.

III. METHODS FOR THE ANALYSIS OF DYNAMIC TAXIING EFFECTS

1. Modal Analysis

Aircraft and their landing equipment form a system with multiple degrees of freedom. In terms of the effects of excitation from the environment, this is expressed by means of the weighted sum from all the modal vibrations of the system. As far as the analysis and measurement of all the nodes in this type of system and their parameters is concerned, that is, modal analysis in the design research on aviation products, automotive vehicles, tractors, and popular conveyances, there have been widespread applications.

Experimental modular analysis is a special type of systems technology. Because of this, it is possible, in an artificial way, to mechanically add vibratory excitation, at the same time measuring the mechanical effects. Using convertor devices, sampling is carried out on the information. After that, it is input into differentiation devices. It goes through FFT transforms, and it is possible to solve for the transmission function between the vibratory excitation points and the effect points. Curves are drawn up for the transmission functions of empirical measurements, and it is possible to learn the modes and modal parameters of the system.

In aviation technology, it is not permissible to release for use a product without going through modal analysis. A good number of engineering departments make use of modern modal analysis technology to set up highly automated experimental analysis systems which are able to quickly carry out modal analysis of parameters, identifying and screening obvious modal vibration forms.
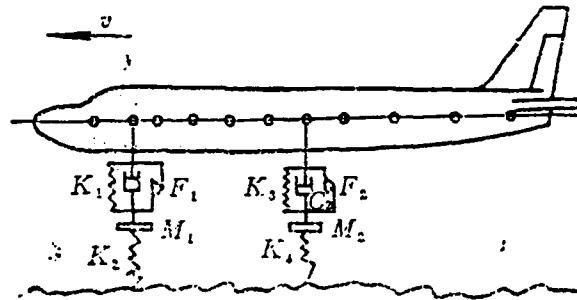
2. Mathematical Analysis Methods

Aircraft can often be described as forming a system with multiple degrees of freedom. In the case of small military aircraft, when designing the taxi spectrum for the take off and landing gear themselves, it is possible to take the fuselage and simplify it into a rigid body. The air springs inside the take off and landing gear cushioning rods and the characteristics of hydraulic damping are capable of supplying linearization or handling on a linear basis according to the principles of energy equivalence. The structures of large aircraft have relatively low frequencies, relatively fast taxi speeds, and relatively large influences from fuselage structural elasticity modalities. If the main take off and landing gear are of the wheel barrow type, it is also necessary to consider the effects from the degree of rotational freedom of the chassis.

As far as an aircraft taxiing at an even speed is concerned, the excitations from the runway are a type of stable random excitation. According to the calculation model in Fig.5, using Newton's Second Law, one can derive the differential equation of motion as follows

$$[M]\{\ddot{q}(t)\}+[C]\{\dot{q}(T)\}+[K]\{q(t)\}$$
$$=\{Q(t)\} \qquad (5)$$

In this equation, [M] is a generalized mass matrix. [C] is
a generalized damping matrix. [K] is a generalized rigidity matrix.
{Q} is a generalized force array. {q} is a generalized coordinate
array. This is a set (including any n) which is capable of completely
describing the coordinates of a system of motion.

Equation (5) is a set of simultaneous second degree ordinary
differential equations, equally applicable to various types of
boundary conditions. However, due to the coupling between the mass,
damping, and rigidity matrices, closed solutions are quite difficult.
It is necessary to go through mathematical methods such as
transformation matrices and so on to make the solutions. If one
selects a set of special coordinates in order to prevent the
appearance of the coupling quantities in the motion equations, that
is, forming a diagonal matrix, makes it possible to make independent
solutions of the non-coupled equation sets. In this, the nature of the
coupling is determined by the generalized coordinates selected for
use, not the basic characteristics of systems with inherent
frequencies.

In order to solve equation (5), take it and rewrite it as

$$\begin{bmatrix} 0 & M \\ M & C \end{bmatrix} \begin{Bmatrix} \ddot{q} \\ \dot{q} \end{Bmatrix} + \begin{bmatrix} -M & 0 \\ 0 & K \end{bmatrix} \begin{Bmatrix} \dot{q} \\ q \end{Bmatrix} = \begin{Bmatrix} 0 \\ Q(t) \end{Bmatrix}$$

(6)

If [M], [C], and [K] are nth order symmetrical matrices, we introduce the 2n+1 order condition or state vector $\{y\} = \begin{Bmatrix} \dot{q} \\ q \end{Bmatrix}$. . Then, equation (6) becomes

$$A\{\dot{y}\} + B\{y\} = \{E(t)\} \qquad (7)$$

We make use of the modal matrix $[\psi]$ to cause the equation(s) above to decouple. We introduce a new condition or state vector $\{Z\}$. Moreover, we make use of the transform below in order to define it, that is

$$\{y\} = [\psi]\{Z\};$$

or

$$\{Z\} = [\psi]^{-1}\{y\} \qquad (8)$$

Equation (7) becomes

$$A[\psi]\{\dot{Z}\} + B[\psi]\{Z\} = \{E(t)\} \qquad (9)$$

We use the transpostion value $[\psi]^{\tau}$ of the modal matrix to multiply equation (9), and we get

$$[A]\{\dot{Z}\} + [B]\{Z\} = [\psi]^{\tau}\{E(t)\}$$
$$= \{N(t)\}$$

In this, [A] and [B] are diagonal matrices, that is

$$a_{ii}\dot{z}_i + b_{ii}z_i = N_i(t) \qquad (i=1,2,\cdots n)$$

58

Its particular or special solution is

$$z_i = \frac{1}{a_{ii}} \int_0^t e^{\gamma_i(t-\tau)} N_i(\tau) dt$$

Its complementary solution is

$$z_i = z_{i_0} e^{\gamma_i t}$$

Its complete solution is

$$z_i = z_{i_0} e^{\gamma_i t} + \frac{1}{a_{ii}} \int_0^t e^{\gamma_i(t-\tau)} N_i(\tau) dt$$

Moreover

$$\begin{bmatrix} \dot{q}(t) \\ q(t) \end{bmatrix} = [\psi]\{Z(t)\}$$

For a complete solution in a generalized coordinate system {q} , it is possible to use the transform of equation (8) in order to make a precise determination, that is

$$\begin{bmatrix} \dot{q}(t) \\ q(t) \end{bmatrix} = \{y(t)\} = [\psi]\{Z(t)\}$$

It should be pointed out that coordinate transformations or transpositions certainly do not change the nature of systems. They only make motion equations easy to solve in order to get answers and nothing more than that.

3. Transmission Function Analysis

In random vibratory systems, for complicated systems of a high order with degrees of freedom in them, it is pcssible to resolve these systems into a problem of solving for the output effects on the basis of transmission functions and input excitations. Excitations can be positional displacements, speeds, accelerations, forces, pressures, and combinations of these things. Output effects can be stress mechanisms, movement processes, and so on.

If the stochastic processes of the excitations are of a normal
distribution, and the system is linear, then, the output effects are
also of a normal distribution. Moreover, it is possible to make
precise determinations from their mean values and mean square values.

In linear systems, the relationship between transmission
functions and the spectra of inputs and outputs is

$$\Phi_0(\omega) = |H(\omega)|^2 \Phi_h(\omega) \qquad (10)$$

In this equation $\Phi_0(\omega)$ is the output spectrum. $H(\omega)$ is the
transmission function. $\Phi_h(\omega)$ is the input spectrum.

The transmission functions can be seen as forming a mathematical
model for the relationship of the inputs and outputs of a physical
system. They can be obtained from theoretical calculations and
empirical measurements. Experimental modal analysis techniques
provide an effective means of measurement in order to get the
transmission functions. Theoretical values and empirical values will
show a certain deviation. At such times, one must continuously adjust
calculations by the use of coefficients in order to make the
theoretical values gradually approach the experimental values over the
entire width of the frequency range. After reaching the hoped for
precision, one can give definite credence to the numerical values of
transmission functions. As far as the calculation of the theoretical
values of transmission functions is concerned, there is often
no real need to solve for the effects in equation (5). For example,
in the case of a simple, single rod take off and landing gear (Fig.6)
with its one degree of system freedom, let us assume that the mass of
the top part of the fuselage is m, that the damping is r, that the air
spring rigidity is K, and that the input from ground surface unevenness
is x(t). Moreover, let us assume that we have stable, ergodic
Gaussian stochastic processes, that the vertical displacement of the
fuselage is y(t), and that the taxi speed is v. According to Newton's
Laws the differential equation of motion is

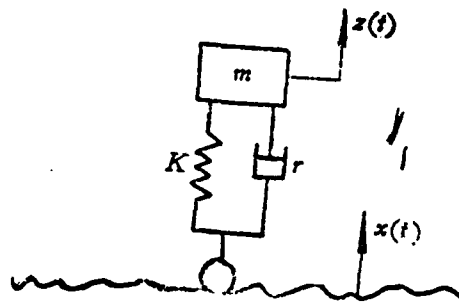$$m z + r \dot{y} + K y = 0 \qquad (11)$$

Fig.6 Diagram of a Take Off and Landing Gear with a Single Degree of Freedom

We already know that

$$z = x + y; \quad \dot{z} = \dot{x} + \dot{y}$$

Then, equation (11) is

$$m\ddot{z} + r\dot{z} + Kz = r\dot{x} + Kx$$

It is possible to carry this a step further and write

$$\ddot{z} + 2\xi\omega_0\dot{z} + \omega_0^2 z = \omega_0^2 f(t)$$

$$(12)$$

In this equation

$$f(t) = \frac{2\xi}{\omega_0}\dot{x} + x$$

This is the equivalent excitation.

61

$$\xi = \frac{r}{(2\sqrt{Km}\,)}$$

$$\omega_0{}^2 = \frac{K}{m}$$

Make the excitation

$$f(t) = Ae^{i\omega t}$$

Then, the effect is

$$z = H(\omega) \cdot Ae^{i\omega t}$$

When one substitutes in equation (12), it is possible to get

$$-\omega^2 H(\omega) + 2i\zeta\omega_0\omega H(\omega) + \omega_0\, H(\omega)$$
$$= \omega_0{}^2$$

Therefore

$$H(\omega) = \frac{1}{\left[1 - \left(\frac{\omega}{\omega_0}\right)^2\right] + 2i\zeta\left(\frac{\omega}{\omega_0}\right)}$$

This H(ω) is, then, the transmission function for the relationship between system input displacement excitations and output effects.

4. The Calculation and Comparison of Random Spectra for Taxiing

In order to present, within a standard model, the curves
describing center of gravity load coefficient excesses for random
loading spectra in taxiing, we will make use of the results above.
For any effect parameter y(x), the normal probability distribution is

$$P(x) = \frac{1}{\sigma_x \sqrt{2\pi}} exp\left[- \frac{(x-\mu_x)^2}{2\sigma_x^2}\right]$$

(13)

In this equation, x is the effect parameter random variable. u_x is
the mean value. σ_x is the standard deviation.

Effects go through analysis. As far as the occurrence number N
for each second over the parameter number u for a certain effect, the
calculation formula is as shown below (4)

$$N(u^*) = \left(\frac{1}{2\pi}\right) e^{-\frac{1}{2}(\frac{u^*}{\sigma})^2} \left[\frac{\int_0^\infty \Omega^2 \cdot \Phi(\Omega) d\Omega}{\int_0^\infty \Phi(\Omega) \cdot d\Omega}\right]$$

(14)

In this equation, N(u) is the occurrence or sequence number for each
second over u^*. $\Phi(.\Omega)$ is the power spectrum. $\hat{\Omega}$ is the time
frequency.

If $u = \Delta n$ (the amount of increase in center of gravity overload),
we can calculate the curves for the excesses of the amounts of
increase in center of gravity overloads for aircraft taxiing on the
ground surface. In Fig.7, one sees presented curves for the U.S.
military standard, the F-100, the F-6, and several kinds of Boeing
aircraft. It is possible to see that, in ranges with large amounts of
increase in overload and relatively low frequencies, large aircraft
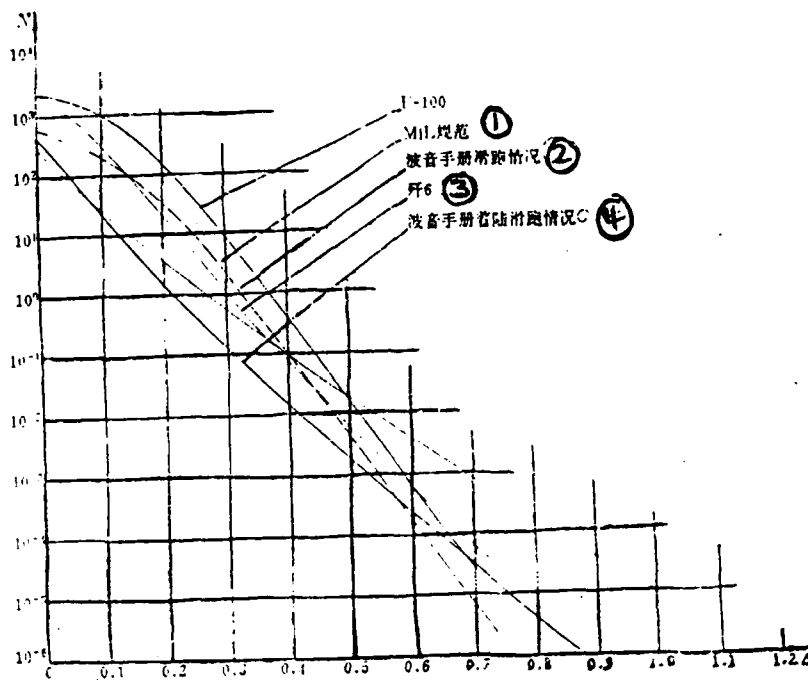had even more severe dynamic effects than small aircraft.

Fig. 7 Table for Amounts of Increase in Center of Gravity Overload
1. MIL Standard   2. Boeing Handbook Taxiing Situation   3. F-6   4.
Boeing Handbook Landing Run Situation C

26

IV. CONCI USION

The uneveness or roughness of airfield runways is a type of
random phenomenon. Speaking of it as a whole, it presents a certain
statistical regularity. The dynamic effects of perturbations or
interference produced in aircraft systems with multiple degrees of
freedom by runway roughness are relatively complicated. For example,
take the elasticity effects of the aircraft, the simplification of
non-linear systems and dynamic models, the solution of high order
differential equations, and so on.   For the last several years,
technical development has been relatively slow. However, in the last

few years, due to computer technology, the quick development of FFT technology, and breakneck progress in random vibration testing techniques, it has already become possible to effectively solve the problems we have described above. In testing and measurements, from sensors, amplification, recording, and analysis, to mathematical processing, everything can be automated. Root mean square values, probability density curves, autocorrelation functions, and power spectrum density functions are all capable of quickly determining measurements. There is no need for complicated calculations. Current software systems are also capable of relatively accurately calculating modal parameters and dynamic effects, as well as other similar quantities.

REFERENCES

(1) Kirk, C.L.and Perry, P.J., Analysis of Taxiing induced Vibrations in Aircraft by the Power Spectral Density Method, The Aeronautical Journal vol.75,No.723,(1971), pp182—194.

(2) Thompson, W.E., Measurements and Power Spectra of Runway Roughness at Airports in Countries of the North Atlantic Treaty Organization, NACA TN-4303 (1958).

(3) Walls, J.H.,Houbolt,J.C. and Harry Press, Some Measurements and Power Spectra of Runway Roughness, NACA TN-2305 (1954).

(4) Grimes, C.K.,Development of a Method and Instrumentation for EvaLuation of Runway Roughness Effects on Military Aircraft, AGARD R-119, (1957).

(5) Coleman, T.L.and Hall, A.W., Implicat- ions of Recent Investigations on Runway Roughness Criteria, AGARD R41 (1963).

THE ANALYSIS FOR DYNAMIC RESPONSE
DURING AIRPLANE TAXIING

Liu   Ruishen   /A88-29257

(*Chengdu Aircratt Company*)

Alstract

A basic method to measure the random variable of runway roughness accord-
ing to roughness criteria based on power spectral concrpts is derived.The power
spectral criteria are primarily used for consideration of aircraft fatigue.

According to the theory of generalized harmonic analysis, the power spect-
ral analysis for random processes must be assumed to be stationary, ergodic and
to agree with Gaussian distribution, On this assumption,a power spectral curve
which provides description of frequency characteristics of roughness for a   run-
way was calculated step by the method decribed in reference 2.

The.we considered the landing gear and its airframe taxiing on the rough
runway as a system with multi-degrees of freedom and derived the simultaneous
differential equations of motion by using Newton's second law.

For simplicity, we used the model matrix as transformation matrix to un-
couple the simultancous differential equations into a set of independent equations

Also,the method of determining transfer function by means of solution of
eigenvalue problems was considered.

At last,the curves of exceedances per flight vs.the incremental accelaration
of airplane during taxiing were introduced.

DISTRIBUTION LIST

DISTRIBUTION DIRECT TO RECIPIENT

ORGANIZATION	MICROFICHE
A205 DMAHTC	1
A210 DMAAC	1
C509 BALLISTIC RES LAB	1
C510 R&T LABS/AVEADCOM	1
C513 ARRADCOM	1
C535 AVRADCOM/TSARCOM	1
C539 TRASANA	1
C591 FSTC	4
C619 MIA REDSTONE	1
D008 MISC	1
E053 HQ USAF/INET	1
E404 AEDC/DOF	1
E408 AFWL	1
E410 AD/IND	1
E429 SD/IND	1
P005 DOE/ISA/DDI	1
P050 CIA/OCR/ADD/SD	2
AFIT/LDE	1
FTD	
CCV	1
MIA/PHS	1
LLYL/CODE L-389	1
NASA/NST-44	1
NSA/T513/TDL	2
ASD/FTD/TQLA	1
FSL/NIX-3	1

FTD-ID(RS)T-0942-88